

Research Article

Gbeminiyi Musibau Sobamowo*

Size-dependent nonlinear vibration analysis of nanobeam embedded in multi-layer elastic media and subjected to electromechanical and thermomagnetic loadings

<https://doi.org/10.1515/cls-2022-0031>

Received Jan 13, 2021; accepted Dec 28, 2021

Abstract: In this work, magneto-electro-mechanical size-dependent nonlinear vibration analysis of nanobeam embedded in multi-layer of Winkler, Pasternak, quadratic and cubic nonlinear elastic media is presented. A nonlinear partial differential equation of motion is derived using Von Karman geometric nonlinearity, nonlocal elasticity theory, Euler-Bernoulli beam theory and Hamilton's principle. Additionally, the efficiency of multiple scales Lindstedt-Poincare method for the strong nonlinear and large amplitude systems is presented. It is established that the results of multiple scales Lindstedt-Poincare method are in good agreements with the numerical and exact solutions for the strong nonlinear problems. However, the classical multiple scales method fails and gives results with very large discrepancies from the results of the numerical and exact solutions when the perturbation parameter is large, and the nonlinearity terms are strong. The high accuracy of the results of multiple scales Lindstedt-Poincare method and its excellent ability to produce accurate results for all values (small and large) of perturbation parameter and the nonlinearity terms show the superiority of the multiple scales Lindstedt-Poincare method over the classical multiple scales method. Further results present the effects of the model parameters on the dynamic behaviour of the nanobeam. It is hoped that the present study will advance nonlinear analysis of the engineering structures.

Keywords: Multiple scales Lindstedt-Poincare method; strongly nonlinear equation; magnetic field; nonlinear vibration; nonlocal elasticity theory

*Corresponding Author: Gbeminiyi Musibau Sobamowo: Department of Mechanical Engineering, University of Lagos, Akoka, Lagos, Nigeria; Department of Mathematics, University of Lagos, Akoka, Lagos, Nigeria; Email: mikegbeminiyiprof@yahoo.com

Nomenclature

A	adimensional maximum amplitude of the nanobeam
E	elastic modulus
E	Young Modulus of Elasticity
EI	bending rigidity
f	axial distributed force
H_x	magnetic field strength
I	moment of area
k	bending strain (curvature)
K	kinetic energy
N	axial force
M	bending moment
k_w	Winkler elastic medium stiffness
k_p	Pasternak elastic medium stiffness
k_2	quadratic nonlinear elastic medium stiffness
k_3	cubic nonlinear elastic medium stiffness
L	length of the nanotube
m_0	mass of the beam per unit length
N	axial/Longitudinal force
N_t	axial thermal load
P	transverse distributed force
r	radius of the nanobeam
ΔT	change in temperature
t	time coordinate
U	strain energy
u	axial displacement of the nanobeam
w	transverse displacement/deflection of the nanobeam
W	work done by the external forces
x	axial coordinate
w_0	initial displacement of nanobeam
$\phi(x)$	trial/comparison function
α_x	coefficient of thermal expansion
η	magnetic field permeability
σ_{xx}	nonlocal normal stresses
$(e_0 a)^2$	nonlocal parameter

ε_{xx} local strain
 ε_{xx}^0 is the extensional strain

1 Introduction

Over the past decades, the applications of nanostructures have been expanding continuously following the discovery of the novel structures by Iijima [1]. In order to gain physical insights and comprehend properties of materials and systems with nanostructures, theoretical mechanics and mechanics of materials have been used to study the static and dynamic behaviours [2–9]. The significance of such studies has been displayed in the ever-increasing applications of nanomaterials in different industrial and engineering systems such as aerospace, advanced reactors, automotive industry, fuel cells turbines, machinery, building and bridge construction, light-weight, low-consumption, developments of nanoelectronics, nanodevices, nanomechanical systems, nanobiological, nanocomposites due to its excellent properties and high strength to weight ratio. and high-sensitivity nanoelectromechanical systems, as well as sensors and composite reinforcements. The excellent mechanical properties such as high elasticity, yield strength, excellent flexibility and conduction have made nanostructures aroused continuous increasing scientific attentions. Also, the nanostructure (Figure 1) undergoes large deformations within the elastic limit and vibrate at frequency in the order of GHz and THz. Consequently, there have been large volumes of research studies that investigated or provided physical insight into the dynamic behaviours of the novel structures [2–9]. In a study on nanostructure, Sears and Batta [10] studied the buckling behaviour of carbon nanotubes subjected to axial compression. Yoon *et al.* [11] explored the noncoaxial resonance of an isolated carbon nanotube with multiple walls while Wang and Cai [13] presented an extended study on the same work with the consideration of the effects of initial stress on the nanostructure. Wang *et al.* [13] analyzed the dynamic behaviour of carbon nanotube with multiple walls using Timoshenko beam model. Zhang *et al.* [14] examined the impact of compressive axial load on the transverse vibrations of carbon nanotube with double walls. Elishakoff and Pentaras [15] presented the fundamental natural frequencies of carbon nanotube with double walls. Buks and Yurke [16] accessed the nonlinear nanomechanical resonator of mass detection while [17] Postma *et al.* [18] determined the dynamic range of carbon nanostructure. Fu *et al.* [18] submitted nonlinear vibration analysis of embedded nanotubes. Vibration of carbon nanotube with electrical actuator was studied by some authors [19–24].

The nonlinear vibrations of the carbon nanotube with double walls were submitted by Hawwa and Al-Qahtani [24]. Hajnaye and Khadem [25] studied the nonlinear dynamic behaviour and stability of the double-walled nanotube subjected to electrostatic actuation. Xu *et al.* [26] considers nonlinear intertube van der Waals forces on the dynamic response of carbon nanotube with double walls. With the aids of nonlocal Timoshenko beam model. Lei *et al.* [27] explored surface effects on the frequency of vibration of carbon nanotube with double walls. Ghorbanpour *et al.* [28] used shell model to analyze nonlinear nonlocal vibration of fluid-conveying embedded carbon nanotubes with double walls.

The analyses of the carbon nanotubes were extended to multi-walled carbon nanotubes (MWCNTs) [29–35]. Sobamowo [36–38], Sobamowo *et al.* [39] as well as Arefi and Nahvi [40] studied nonlinear vibration in nanostructures with slightly and initial curvature while Cigeroglu and Samandari [41] analyzed the dynamic behaviour of curved nanobeams.

Studies on vibrations of nanotubes as presented in literatures using experimental measurements, density functional theory, molecular dynamics simulations, and classical continuum theories and non-classical continuum theories such as nonlocal stress theory, modified couple stress theory, gradient strain theory, and surface elasticity theory. There are some difficulties in the experiment investigations at the nanoscale level. Therefore, majority of the past works are based on theoretical investigations using classical continuum models (which do not consider the small-scale effects). However, due to their scale-free models as they cannot incorporate the small-scale effects in their formulations, the classical continuum theories are inadequate for the accurate predictions of the dynamic behaviours of the nanotubes. Such inadequacy in the classical continuum models is corrected in the works of Eringen [42–44] and that of Eringen and Edelen [45], where the author developed nonlocal continuum mechanics based on nonlocal elasticity theory. Although, some studies in literature have used the nonlocal continuum mechanics to present some theoretical investigations [46–71]. Simsek [72] as well as Murmu and Pradhan [73] adopted nonlocal elasticity theory to study the nonlinear vibration of a carbon nanotube embedded in an elastic medium. In a recent study, Abdullah *et al.* [74] presented effects of temperature, magnetic field, and elastic media on the nonlinear vibration of nanobeams. The authors present very good work and results. However, the dynamic response of the nanobeam was not fully explored and the effect of electric field on the vibration characteristics of the nanobeam was not studied. Moreover, to the best of the authors knowledge, a study on

the effects of electromechanical and thermomagnetic loadings on the nonlinear vibration of nanobeams embedded in Winkler, Pasternak, quadratic and cubic nonlinear elastic media has not been presented in literature. Additionally, the past studies did not explore the efficacy of multiple scales Lindstedt-Poincaré method for the strong nonlinear and large amplitude systems. Therefore, with the aid of multiple scales Lindstedt-Poincaré method, the present work developed analytical solutions for magneto-electromechanical size-dependent nonlinear vibration analysis of nanobeam embedded in multi-layer of Winkler, Pasternak, quadratic and cubic nonlinear elastic media. With the considerations of Von Karman geometric nonlinearity effect and with the aids of nonlocal elasticity theory and Euler-Bernoulli beam model, the equation of motion for the nanobeam is derived using Hamilton's principle. Also, the present analysis used four layers (Winkler, Pasternak, and quadratic and cubic nonlinear layers) which generate nonlinearities in the developed dynamic models. Additionally, the impacts of nonlocal parameter, electromechanical parameter, magnetic force, elastic media, temperature, and amplitude on the dynamic behaviour of the nanotube are investigated.

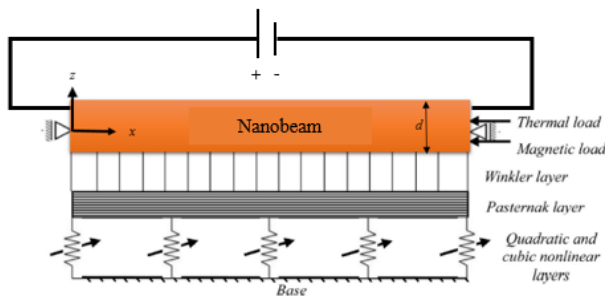


Figure 1: A piezoelectric nanobeam embedded in linear and nonlinear elastic media. (Note: only the bottom side of the elastic media is shown)

2 Model development for the single-walled nanotube

Consider a nanobeam embedded in linear and nonlinear elastic media as shown in Figure 1. The nanobeam is subjected to stretching effects and resting on Winkler, Pasternak and nonlinear elastic media in a thermo-magnetic environment as depicted in the figure.

Applying the nonlocal theory presented by Eringen [42–44], Eringen and Edelen [45] and Euler-Bernoulli beam theorem, the following governing equation is developed

$$\begin{aligned} EI \left(\frac{\partial^4 \bar{w}}{\partial \bar{x}^4} \right) + \rho A_c \frac{\partial^2}{\partial t^2} \left[\bar{w} - (e_0 a)^2 \frac{\partial^2 \bar{w}}{\partial \bar{x}^2} \right] & \quad (1) \\ + k_w \left[\bar{w} - (e_0 a)^2 \frac{\partial^2 \bar{w}}{\partial \bar{x}^2} \right] - k_p \frac{\partial^2}{\partial \bar{x}^2} \left[\bar{w} - (e_0 a)^2 \frac{\partial^2 \bar{w}}{\partial \bar{x}^2} \right] \\ + k_2 \left[\bar{w}^2 - (e_0 a)^2 \frac{\partial^2 (\bar{w}^2)}{\partial \bar{x}^2} \right] + k_3 \left[\bar{w}^3 - (e_0 a)^2 \frac{\partial^2 (\bar{w}^3)}{\partial \bar{x}^2} \right] \\ - \eta A_c H_x^2 \frac{\partial^2}{\partial \bar{x}^2} \left[\bar{w} - (e_0 a)^2 \frac{\partial^2 \bar{w}}{\partial \bar{x}^2} \right] \\ + \left(EA_c \frac{\alpha_x \Delta T}{1 - 2\nu} \right) \frac{\partial^2}{\partial \bar{x}^2} \left[\bar{w} - (e_0 a)^2 \frac{\partial^2 \bar{w}}{\partial \bar{x}^2} \right] \\ + \zeta E_z A_c \frac{\partial^2}{\partial \bar{x}^2} \left[\bar{w} - (e_0 a)^2 \frac{\partial^2 \bar{w}}{\partial \bar{x}^2} \right] \\ - \left[\left(\frac{EA_c}{2L} \int_0^L \left(\frac{\partial \bar{w}}{\partial \bar{x}} \right)^2 d\bar{x} \right) \left(\frac{\partial^2 \bar{w}}{\partial \bar{x}^2} - (e_0 a)^2 \frac{\partial^4 \bar{w}}{\partial \bar{x}^4} \right) \right] = 0 \end{aligned}$$

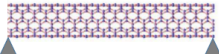
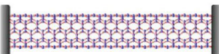
The derivation can be found in the Appendix.

It is assumed that the midpoint of the nanobeam is subjected to the following initial conditions

$$\bar{w}(\bar{x}, 0) = \bar{w}_0, \quad \frac{\partial^2 \bar{w}(\bar{x}, 0)}{\partial^2 \bar{x}} = 0 \quad (2)$$

The following boundary conditions for the multi-walled nanotubes are considered in this work:

Table 1: The basic functions corresponding to the above boundary conditions

Cases	Mode shape, $\phi(x)$	Value of β for the first mode
1. Simply support 	$\sin\left(\frac{\beta x}{L}\right)$	π
2. Clamped-Clamped support or 	$\left(\cosh\left(\frac{\beta x}{L}\right) - \cos\left(\frac{\beta x}{L}\right) \right) - \left(\frac{\sinh \beta + \sin \beta}{\cosh \beta - \cos \beta} \right) \left(\sinh\left(\frac{\beta x}{L}\right) - \sin\left(\frac{\beta x}{L}\right) \right)$ or $\frac{1}{2} \left(1 - \cos\left(\frac{\beta x}{L}\right) \right)$	4.730041 2 π

For simply supported (S-S) nanotube,

$$\begin{aligned}\bar{w}(0, \bar{t}) = 0, \quad \frac{\partial^2 \bar{w}(0, \bar{t})}{\partial^2 \bar{x}} = 0, \quad \bar{w}(L, \bar{t}) = 0, \\ \frac{\partial^2 \bar{w}(L, \bar{t})}{\partial^2 \bar{x}} = 0.\end{aligned}\quad (3)$$

For clamped-clamped supported (C-C) nanotube,

$$\begin{aligned}\bar{w}(0, \bar{t}) = 0, \quad \frac{\partial \bar{w}(0, \bar{t})}{\partial \bar{x}} = 0, \\ \bar{w}(L, \bar{t}) = 0, \quad \frac{\partial \bar{w}(L, \bar{t})}{\partial \bar{x}} = 0.\end{aligned}\quad (4)$$

Using the following adimensional constants and variables

$$\begin{aligned}x = \frac{\bar{x}}{L}; \quad w = \frac{\bar{w}}{r}; \quad t = \sqrt{\frac{EI}{\rho A_c L^4}}; \quad r = \sqrt{\frac{I}{A_c}}; \\ h = \frac{e_0 a}{L}; \quad \alpha_t^d = \frac{N_{thermal} L^2}{EI}; \quad A = \frac{\bar{w}_0}{r}; \\ \xi_e = \frac{\zeta E_z A_c L^2}{EI}; \quad K_w = \frac{k_w L^4}{EI}; \quad K_p = \frac{k_p L^2}{EI}; \\ Ha_m = \frac{\eta A_c H_x^2 L^2}{EI}; \quad K_2^d = \frac{k_2 r L^4}{EI}; \quad K_3^d = \frac{k_3 r^2 L^4}{EI}.\end{aligned}\quad (5)$$

The adimensional form of the governing equation of motion for the nanobeam is given as

$$\begin{aligned}\left[1 + K_p h^2 + Ha_m h^2 - \alpha_t^d h^2 - \xi_e h^2 \right. \\ \left. + \frac{h^2}{2} \int_0^1 \left(\frac{\partial w}{\partial x} \right)^2 dx \right] \frac{\partial^4 w}{\partial x^4} + \left[\alpha_t^d + \xi_e - K_w h^2 - K_p - Ha_m \right. \\ \left. - \frac{1}{2} \int_0^1 \left(\frac{\partial w}{\partial x} \right)^2 dx \right] \frac{\partial^2 w}{\partial x^2} + K_w w + \frac{\partial^2 w}{\partial t^2} - h^2 \frac{\partial^4 w}{\partial x^2 \partial t^2} \\ \left. + K_2^d \left[w^2 - h^2 \frac{\partial^2 (w^2)}{\partial x^2} \right] + K_3^d \left[w^3 - h^2 \frac{\partial^2 (w^3)}{\partial x^2} \right] = 0\end{aligned}\quad (6)$$

And the boundary conditions become

For simply supported (S-S) nanotube,

$$\begin{aligned}w(0, t) = 0, \quad \frac{\partial^2 w(0, t)}{\partial x^2} = 0, \\ w(1, t) = 0, \quad \frac{\partial^2 w(1, t)}{\partial x^2} = 0.\end{aligned}\quad (7)$$

For clamped-clamped supported (C-C) nanotube,

$$\begin{aligned}w(0, t) = 0, \quad \frac{\partial w(0, t)}{\partial x} = 0, \\ w(1, t) = 0, \quad \frac{\partial w(1, t)}{\partial x} = 0.\end{aligned}\quad (8)$$

treatment technique. As the name implies the Galerkin decomposition method is used to decompose the governing partial differential equation of motion can be separated into spatial and temporal parts. The resulting temporal equations are solved using multiple scales Lindstedt-Poincare method. The procedures for the analysis of the equations are given in the proceeding sections as follows:

3.1 Galerkin decomposition method

With the application of Galerkin decomposition procedure, the governing partial differential equations of motion can be separated into spatial and temporal parts of the lateral displacement function as

$$w(x, t) = \phi(x) q(t) \quad (9)$$

Using one-parameter Galerkin decomposition procedure, one arrives at

$$\int_0^1 R(x, t) \phi(x) dx = 0 \quad (10)$$

where is $R(x, t)$ the governing equation of motion for nanobeam i.e.

$$\begin{aligned}R(x, t) = \left[1 + K_p h^2 + Ha_m h^2 - \alpha_t^d h^2 \right. \\ \left. + \frac{h^2}{2} \int_0^1 \left(\frac{\partial w}{\partial x} \right)^2 dx \right] \frac{\partial^4 w}{\partial x^4} + \left[\alpha_t^d - K_w h^2 - K_p \right. \\ \left. - Ha_m - \frac{1}{2} \int_0^1 \left(\frac{\partial w}{\partial x} \right)^2 dx \right] \frac{\partial^2 w}{\partial x^2} + K_w w + \frac{\partial^2 w}{\partial t^2} \\ \left. - h^2 \frac{\partial^4 w}{\partial x^2 \partial t^2} + K_2^d \left[w^2 - h^2 \frac{\partial^2 (w^2)}{\partial x^2} \right] \right. \\ \left. + K_3^d \left[w^3 - h^2 \frac{\partial^2 (w^3)}{\partial x^2} \right] = 0\end{aligned}\quad (11)$$

where $\phi(x)$ is the basis or trial or comparison function or normal function, which must satisfy the kinetic boundary conditions in Eqs. (7) and (8), and $q(t)$ is the temporal part (time-dependent function).

Substituting Eqs. (11) into (10), then multiplying both sides of the resulting equation by $\phi(x)$ and integrating it

3 Methods of solution

The methods of solution for the governing equation include Galerkin decomposition, power series method and after-

for the domain of $(0, 1)$

$$\int_0^1 \left\{ \begin{aligned} & \left[1 + K_p h^2 + H a_m h^2 \right. \\ & \quad \left. - \alpha_t^d h^2 + \frac{h^2}{2} \int_0^1 \left(\frac{\partial w}{\partial x} \right)^2 dx \right] \frac{\partial^4 w}{\partial x^4} \\ & + \left[\alpha_t^d - K_w h^2 - K_p - H a_m \right. \\ & \quad \left. - \frac{1}{2} \int_0^1 \left(\frac{\partial w}{\partial x} \right)^2 dx \right] \frac{\partial^2 w}{\partial x^2} + K_w w + \frac{\partial^2 w}{\partial t^2} \\ & - h^2 \frac{\partial^4 w}{\partial x^2 \partial t^2} + K_2^d \left[w^2 - h^2 \frac{\partial^2 (w^2)}{\partial x^2} \right] \\ & + K_3^d \left[w^3 - h^2 \frac{\partial^2 (w^3)}{\partial x^2} \right] \end{aligned} \right\} \phi(x) dx = 0 \quad (12)$$

Substitution of Eq. (9) into Eq. (12), gives

$$\int_0^1 \left\{ \begin{aligned} & \left[1 + K_p h^2 + H a_m h^2 - \alpha_t^d h^2 \right. \\ & \quad \left. + \frac{h^2}{2} \int_0^1 \left(\frac{\partial(\phi(x)q(t))}{\partial x} \right)^2 dx \right] \frac{\partial^4(\phi(x)q(t))}{\partial x^4} \\ & + \left[\alpha_t^d - K_w h^2 - K_p - H a_m \right. \\ & \quad \left. - \frac{1}{2} \int_0^1 \left(\frac{\partial(\phi(x)q(t))}{\partial x} \right)^2 dx \right] \frac{\partial^2(\phi(x)q(t))}{\partial x^2} \\ & + K_w (\phi(x)q(t)) + \frac{\partial^2(\phi(x)q(t))}{\partial t^2} \\ & - h^2 \frac{\partial^4(\phi(x)q(t))}{\partial x^2 \partial t^2} \\ & + K_2^d \left[(\phi(x)q(t))^2 \right. \\ & \quad \left. - h^2 \frac{\partial^2((\phi(x)q(t))^2)}{\partial x^2} \right] \\ & + K_3^d \left[(\phi(x)q(t))^3 \right. \\ & \quad \left. - h^2 \frac{\partial^2((\phi(x)q(t))^3)}{\partial x^2} \right] \end{aligned} \right\} \phi(x) dx = 0 \quad (13)$$

$$\int_0^1 \left\{ \begin{aligned} & \left[1 + K_p h^2 + H a_m h^2 - \alpha_t^d h^2 \right. \\ & \quad \left. + \frac{h^2 q^2(t)}{2} \int_0^1 \left(\frac{\partial \phi(x)}{\partial x} \right)^2 dx \right] q(t) \frac{\partial^4 \phi(x)}{\partial x^4} \\ & + \left[\alpha_t^d - K_w h^2 - K_p - H a_m \right. \\ & \quad \left. - \frac{q^2(t)}{2} \int_0^1 \left(\frac{\partial \phi(x)}{\partial x} \right)^2 dx \right] q(t) \frac{\partial^2 \phi(x)}{\partial x^2} \\ & + K_w (\phi(x)q(t)) + \phi(x) \frac{\partial^2 q(t)}{\partial t^2} \\ & - h^2 \left(\frac{\partial^2}{\partial x^2} \left(\phi(x) \frac{\partial^2 q(t)}{\partial t^2} \right) \right) \\ & + K_2^d \left[(\phi(x)q(t))^2 \right. \\ & \quad \left. - h^2 q^2(t) \frac{\partial^2((\phi(x))^2)}{\partial x^2} \right] \\ & + K_3^d \left[(\phi(x)q(t))^3 \right. \\ & \quad \left. - h^2 q^3(t) \frac{\partial^2((\phi(x))^3)}{\partial x^2} \right] \end{aligned} \right\} \phi(x) dx = 0 \quad (14)$$

$$\int_0^1 \left\{ \begin{aligned} & \left[1 + K_p h^2 + H a_m h^2 - \alpha_t^d h^2 \right. \\ & \quad \left. + \frac{h^2 q^3(t)}{2} \int_0^1 \left(\frac{\partial \phi(x)}{\partial x} \right)^2 dx \right] \frac{\partial^4 \phi(x)}{\partial x^4} \\ & + \left[\alpha_t^d - K_w h^2 - K_p - H a_m \right. \\ & \quad \left. - \frac{q^3(t)}{2} \int_0^1 \left(\frac{\partial \phi(x)}{\partial x} \right)^2 dx \right] \frac{\partial^2 \phi(x)}{\partial x^2} \\ & + K_w (\phi(x)q(t)) + \phi(x) \frac{\partial^2 q(t)}{\partial t^2} \\ & - h^2 \left(\frac{\partial^2 q(t)}{\partial t^2} \frac{\partial^2 \phi(x)}{\partial x^2} \right) \\ & + K_2^d \left[(\phi(x)q(t))^2 \right. \\ & \quad \left. - h^2 q^2(t) \frac{\partial^2((\phi(x))^2)}{\partial x^2} \right] \\ & + K_3^d \left[(\phi(x)q(t))^3 \right. \\ & \quad \left. - h^2 q^3(t) \frac{\partial^2((\phi(x))^3)}{\partial x^2} \right] \end{aligned} \right\} \phi(x) dx = 0 \quad (15)$$

$$\int_0^1 \left\{ \begin{aligned} & \left[\phi^2(x) - h^2 \phi(x) \left(\frac{\partial^2 \phi(x)}{\partial x^2} \right) \right] \frac{\partial^2 q(t)}{\partial t^2} \\ & + \left[\begin{aligned} & K_w \phi^2(x) + (1 + K_p h^2 \\ & + H a_m h^2 - \alpha_t^d h^2) \phi(x) \frac{\partial^4 \phi(x)}{\partial x^4} \\ & + ((\alpha_t^d - K_w h^2 - K_p \\ & - H a_m) \phi(x) \frac{\partial^2 \phi(x)}{\partial x^2}) \end{aligned} \right] q(t) \\ & + K_2^d \left[\phi^3(x) - h^2 \phi(x) \frac{\partial^2 ((\phi(x))^2)}{\partial x^2} \right] q^2(t) \\ & + \left[\begin{aligned} & K_3^d \left[\phi^4(x) - h^2 \phi(x) \frac{\partial^2 ((\phi(x))^3)}{\partial x^2} \right] \\ & + \left(\left[\frac{h^2}{2} \int_0^1 \left(\frac{\partial \phi(x)}{\partial x} \right)^2 dx \right] \phi(x) \frac{\partial^4 \phi(x)}{\partial x^4} \right) \\ & - \left(\left[\frac{1}{2} \int_0^1 \left(\frac{\partial \phi(x)}{\partial x} \right)^2 dx \right] \phi(x) \frac{\partial^2 \phi(x)}{\partial x^2} \right) \end{aligned} \right] q^3(t) \end{aligned} \right\} dx = 0 \quad (16)$$

Therefore, Eq. (16) can be written as

$$\overline{\lambda_0} \frac{d^2 q(t)}{dt^2} + \overline{\lambda_1} q(t) + \overline{\lambda_2} q^2(t) + \overline{\lambda_3} q^3(t) = 0 \quad (17)$$

Furthermore, we can express Eq. (62) as

$$\frac{d^2 q(t)}{dt^2} + \lambda_1 q(t) + \lambda_2 q^2(t) + \lambda_3 q^3(t) = 0 \quad (18)$$

where

$$\lambda_1 = \frac{\overline{\lambda_1}}{\overline{\lambda_0}}; \quad \lambda_2 = \frac{\overline{\lambda_2}}{\overline{\lambda_0}}; \quad \lambda_3 = \frac{\overline{\lambda_3}}{\overline{\lambda_0}}; \quad (19)$$

$$\overline{\lambda_0} = \int_0^1 \left(\phi^2 - h^2 \phi \frac{\partial^2 \phi}{\partial x^2} \right) dx \quad (20)$$

$$\begin{aligned} \overline{\lambda_1} = \int_0^1 & \left(K_w \phi^2 + (1 + K_p h^2 + H a_m h^2 \right. \\ & \left. - \alpha_t^d h^2) \phi \frac{\partial^4 \phi}{\partial x^4} + (\alpha_t^d - K_w h^2 - K_p - H a_m) \phi \frac{\partial^2 \phi}{\partial x^2} \right) dx \end{aligned} \quad (21)$$

$$\overline{\lambda_2} = \int_0^1 K_2^d \left(\phi^3 - h^2 \phi \frac{\partial^2 (\phi^2)}{\partial x^2} \right) dx \quad (22)$$

$$\begin{aligned} \overline{\lambda_3} = \int_0^1 & K_3^d \left(\phi^4 - h^2 \phi \frac{\partial^2 (\phi^3)}{\partial x^2} \right) dx \\ & + \frac{h^2}{2} \int_0^1 \left(\frac{\partial \phi}{\partial x} \right)^2 dx \int_0^1 \phi \frac{\partial^2 \phi}{\partial x^2} dx \\ & - \frac{1}{2} \int_0^1 \left(\frac{\partial \phi}{\partial x} \right)^2 dx \int_0^1 \phi \frac{\partial^4 \phi}{\partial x^4} dx \end{aligned} \quad (23)$$

The initial conditions are given as

$$q(0) = a_0, \quad \frac{dq(0)}{dt} = 0 \quad (24)$$

a_0 is the maximum vibration amplitude of the structure.

3.2 Method of solution: Multiple scales Lindstedt-Poincare method

It can be seen from the above procedures that the apart from the fact that the Galerkin decomposition method decomposes governing equation of motion into spatial and temporal parts, it also helps in converting the space- and time-dependent partial differential equation to a time-dependent ordinary differential equation. The nonlinear ordinary differential equation easily be solved using numerical methods or approximate analytical methods. In this work, multiple scales Lindstedt-Poincare method (MSLPM) is adopted due to its ability of providing convergent solutions for large perturbation parameters, strong nonlinearities, and development of total analytic solution with good accuracy.

Multiple scales Lindstedt-Poincare method is a modified multiple scales method which incorporates the time transformation of Lindstedt-Poincare method [75–80]. One of the major advantages of the multiple scales method over the Lindstedt-Poincare method is that transient solutions can be found using the multiple scales method whereas it is impossible to retrieve such solutions using the Lindstedt-Poincare method. Combining both multiple scales and Lindstedt-Poincare methods as it is achieved in the multiple scales Lindstedt-Poincare method would augment the advantages of methods in the multiple scales Lindstedt-Poincare method so that both steady state and transient solutions with improved convergence properties can be achieved. Also, by expanding the natural frequency in the modified Lindstedt-Poincare method, convergent solutions for large values of perturbation parameters and strong nonlinearities are possible.

3.2.1 Determination of natural frequencies

In order to find out the natural frequencies of the structure, the following analysis are carried out:

The nonlinearity and excitation are ordered so that they appear at the same time in the perturbation scheme. Therefore, take λ_2 and λ_3 as $\varepsilon \tilde{\lambda}_2$ and $\varepsilon \tilde{\lambda}_3$. Applying the first transformation, $\tau = \omega t$, to Eq. (18), one arrives at

$$\omega^2 q'' + \omega_0 q + \varepsilon \tilde{\lambda}_2 q^2 + \varepsilon^2 \tilde{\lambda}_3 q^3 = 0 \quad (25)$$

where prime denotes derivative with respect to the new time variable τ and $\lambda_1 = \omega_0$ is the linear frequency of the system. It should be stated that fast and slow time scales are slightly different in the multiple scales Lindstedt-Poincare method. The fast and slow time scales are defined as

$$T_0 = \tau, \quad T_1 = \varepsilon \tau, \quad T_2 = \varepsilon^2 \tau \quad (26)$$

Therefore, the first and second derivatives are expressed as

$$\frac{d}{d\tau} = D_0 + \varepsilon D_1 + \varepsilon^2 D_2 + \dots \quad (27)$$

$$\frac{d^2}{d\tau^2} = D_0^2 + 2\varepsilon D_0 D_1 + \varepsilon^2 (D_1^2 + 2D_0 D_2) + \dots \quad (28)$$

where

$$D_n = \frac{\partial}{\partial T_n}$$

Assuming that the solution of Eq. (25) can be expressed as

$$q = q_0(T_0, T_1, T_2) + \varepsilon q_1(T_0, T_1, T_2) + \varepsilon^2 q_2(T_0, T_1, T_2) + \dots \quad (29)$$

and

$$\omega^2 = \omega_0 + \varepsilon \omega_1 + \varepsilon^2 \omega_2 + \dots \quad (30)$$

From Eq. (29), one can write that

$$\omega_0 = \omega^2 - \varepsilon \omega_1 - \varepsilon^2 \omega_2 + \dots \quad (31)$$

Substitute Eqs. (29) and (31) into Eq. (25), gives the following

$$\begin{aligned} & \omega^2 (D_0^2 + 2\varepsilon D_0 D_1 + \varepsilon^2 (D_1^2 + 2D_0 D_2) + \dots) (q_0(T_0, T_1, T_2) + \varepsilon q_1(T_0, T_1, T_2) + \varepsilon^2 q_2(T_0, T_1, T_2) + \dots) \\ & + (\omega^2 - \varepsilon \omega_1 - \varepsilon^2 \omega_2 + \dots) (q_0(T_0, T_1, T_2) + \varepsilon q_1(T_0, T_1, T_2) + \varepsilon^2 q_2(T_0, T_1, T_2) + \dots) \\ & + \varepsilon \lambda_2 (q_0(T_0, T_1, T_2) + \varepsilon q_1(T_0, T_1, T_2) + \varepsilon^2 q_2(T_0, T_1, T_2) + \dots)^2 \\ & + \varepsilon \lambda_3 (q_0(T_0, T_1, T_2) + \varepsilon q_1(T_0, T_1, T_2) + \varepsilon^2 q_2(T_0, T_1, T_2) + \dots)^3 = 0 \end{aligned} \quad (32)$$

Also, for the initial conditions in Eq. (24), one has

$$q_0(0, 0, 0) + \varepsilon q_1(0, 0, 0) + \varepsilon^2 q_2(0, 0, 0) + \dots = a_0, \quad (33)$$

$$\begin{aligned} & \frac{d(q_0(0, 0, 0) + \varepsilon q_1(0, 0, 0) + \varepsilon^2 q_2(0, 0, 0) + \dots)}{d\tau} \\ & = (D_0 + \varepsilon D_1 + \varepsilon^2 D_2 + \dots) (q_0(0, 0, 0) + \varepsilon q_1(0, 0, 0) + \varepsilon^2 q_2(0, 0, 0) + \dots) = 0 \end{aligned} \quad (34)$$

Arranging Eqs. (32), (33) and (34) according to the powers of the perturbation parameter ε , gives

The zeroth-order equation is

$$\varepsilon^0 : quad \omega^2 D_0^2 q_0 + \omega^2 q_0 = 0 \quad (35)$$

The initial conditions are

$$q_0(0) = A, \quad D_0 q_0(0) = 0 \quad (36)$$

The first-order equation is

$$\varepsilon^1 : \quad \omega^2 D_0^2 q_1 + \omega^2 q_1 = -2\omega^2 D_0 D_1 q_0 + \omega_1 q_0 - \tilde{\lambda}_2 q_0^2 \quad (37)$$

The initial conditions are

$$q_1(0) = 0, \quad D_0 q_1(0) + D_1 q_0(0) = 0 \quad (38)$$

The second-order equation is

$$\begin{aligned} \varepsilon^2 : \quad & \omega^2 D_0^2 q_2 + \omega^2 q_2 = -2\omega^2 D_0 D_1 q_1 \\ & - \omega_2 (D_1^2 + 2D_0 D_2) q_0 + \omega_2 q_1 + \omega_2 q_0 - 2\tilde{\lambda}_2 q_0 q_1 \\ & - \tilde{\lambda}_3 q_0^3 \end{aligned} \quad (39)$$

The initial conditions are

$$q_2(0) = 0, \quad D_0 q_2(0) + D_1 q_1(0) + D_2 q_0(0) = 0 \quad (40)$$

The solution of the zeroth-order is

$$q_0 = A(T_1, T_2) e^{iT_0} + cc, \quad (41)$$

where cc stands for the complex conjugates and A is given by the following polar form.

$$A = \frac{1}{2} \tilde{a} e^{i\beta}, \quad (42)$$

The solution in Eq. (41) can be written in real form as

$$q_0 = \tilde{a} \cos(T_0 + \beta), \quad (43)$$

Applying the initial conditions, provides

$$\tilde{a}(0) = a_0, \quad \beta(0) = 0 \quad (44)$$

Substituting Eq. (43) into Eq. (39) and eliminating the secularities require that

$$-2i\omega^2 D_1 A + \omega_1 A = 0 \quad (45)$$

Without loss of generality, selecting $D_1 A = 0$, it implies that

$$a = \tilde{a}(T_2), \quad \beta = \beta(T_2) \quad \text{and} \quad \omega_1 = 0 \quad (46)$$

The solution of the first-order is given as

$$q_1 = B(T_1, T_2) e^{iT_0} + cc \quad (47)$$

$$+ \frac{1}{3\omega^2} \alpha_1 \left(A^2 e^{2iT_0} + cc - 6A\bar{A} \right)$$

where

$$B = \frac{1}{2} \tilde{b} e^{i\gamma},$$

Alternatively, the real form of q_1 is given as

$$q_1 = b \cos(T_0 + \gamma) + cc \quad (48)$$

$$+ \frac{1}{6\omega^2} \tilde{\lambda}_2 a^2 (\cos(2T_0 + 2\beta) - 3)$$

The initial conditions at the first order imply that

$$b(0) = \frac{1}{3\omega^2} \tilde{\lambda}_2 a_0^2, \quad \gamma(0) = 0 \quad (49)$$

For the second/last order, on substituting Eq. (47) and (41) into (39) and eliminating the secular terms, produces

$$-2i\omega^2 D_1 B - 2i\omega^2 D_2 A + \omega_2 A \quad (50)$$

$$+ \left(\frac{10}{3\omega^2} \tilde{\lambda}_2^2 - 3\tilde{\lambda}_3 \right) A^2 \tilde{A} = 0$$

Also, without loss of generality, $D_1 B = 0$, can be selected. However, according to MSLPM, $D_1 A = 0$ should be tried. The choice makes a real ω_2 and therefore admissible. After the algebraic manipulation, it was found that

$$a = a_0, \quad b(0) = \frac{1}{3\omega^2} \tilde{\lambda}_2 a_0^2, \quad (51)$$

$$\beta = \gamma = 0, \quad \omega_2 = a_0^2 \left(\frac{3}{4} \tilde{\lambda}_3 - \frac{5}{6\omega^2} \tilde{\lambda}_2^2 \right)$$

Substituting (46) and (51) into Eq. (30), the frequency of vibration is given as

$$\omega^2 = \omega_0^2 + \varepsilon^2 a_0^2 \left(\frac{3}{4} \tilde{\lambda}_3 - \frac{5}{6\omega^2} \tilde{\lambda}_2^2 \right) \quad (52)$$

It should be noted that ω^2 appears on both RHS and LHS of Eq. (52), therefore, solving for real and positive value of ω^2 results in

$$\omega^2 = \omega_0^2 \left[\frac{1}{2} \left(1 + \frac{3\varepsilon^2 a_0^2 \tilde{\lambda}_3}{4\omega_0^2} \right) \right. \quad (53)$$

$$\left. + \sqrt{\frac{1}{2} \left(1 + \frac{3\varepsilon^2 a_0^2 \tilde{\lambda}_3}{4\omega_0^2} \right)^2 - \frac{10\varepsilon^2 a_0^2 \tilde{\lambda}_2}{3\omega_0^4}} \right]$$

Which can be written as

$$\omega = \omega_0 \sqrt{\frac{1}{2} \left(1 + \frac{3\varepsilon^2 a_0^2 \tilde{\lambda}_3}{4\omega_0^2} \right) + \sqrt{\frac{1}{2} \left(1 + \frac{3\varepsilon^2 a_0^2 \tilde{\lambda}_3}{4\omega_0^2} \right)^2 - \frac{10\varepsilon^2 a_0^2 \tilde{\lambda}_2}{3\omega_0^4}}} \quad (54)$$

The frequency ratio, $\psi = \frac{\omega}{\omega_0}$ (ratio of the linear to nonlinear frequency) is given as

$$\psi = \sqrt{\frac{1}{2} \left(1 + \frac{3\varepsilon^2 a_0^2 \tilde{\lambda}_3}{4\omega_0^2} \right) + \sqrt{\frac{1}{2} \left(1 + \frac{3\varepsilon^2 a_0^2 \tilde{\lambda}_3}{4\omega_0^2} \right)^2 - \frac{10\varepsilon^2 a_0^2 \tilde{\lambda}_2}{3\omega_0^4}}} \quad (55)$$

The final solution in terms of the nonlinear frequency is given as

$$q = a_0 \cos(\omega t) + \frac{\varepsilon \tilde{\lambda}_2 a_0^2}{6\omega^2} (2\cos(\omega t) + \cos(2\omega t) - 3) \quad (56)$$

$$+ O(\varepsilon^2)$$

3.2.2 Validation of the solution of the multiple scales Lindstedt-Poincare method

On invoking the well-known perturbation criteria, the correction terms must be much smaller than the leading terms for solution to be valid. Therefore, for the above solution in Eq. (56) to be valid,

$$\frac{\varepsilon \tilde{\lambda}_2 a_0^2}{6\omega^2} \ll 1 \quad (57)$$

The analysis for the proof of validity is given as

$$\lim_{\varepsilon \rightarrow \infty} \frac{\varepsilon \tilde{\lambda}_2 a_0}{6\omega^2} = \lim_{\varepsilon \rightarrow \infty} \frac{\varepsilon \tilde{\lambda}_2 a_0}{6[A]} = 0 \ll 1 \quad (58)$$

where

$$A = \frac{1}{2} \left(1 + \frac{3\varepsilon^2 a_0^2 \tilde{\lambda}_3}{4\omega_0^2} \right)$$

$$+ \sqrt{\frac{1}{2} \left(1 + \frac{3\varepsilon^2 a_0^2 \tilde{\lambda}_3}{4\omega_0^2} \right)^2 - \frac{10\varepsilon^2 a_0^2 \tilde{\lambda}_2}{3\omega_0^4}}$$

It is shown that the correction term (the second term) in Eq. (56) is always a small quantity compared with the leading term which assures convergence. The analysis presented in Eq. (58) for the solution provided by the multiple scales Lindstedt-Poincare method shows that solution will always converge for all values of perturbation parameters, ε and strong nonlinearity terms ($\tilde{\lambda}_2$ and $\tilde{\lambda}_3$). This is demonstrated in Table 2 and 3 as well as the figures in the results and discussion sections.

3.2.3 Analytical solution using Multiple scales method

With the application of classical multiple scales method is applied, the developed analytical solution is

$$q = a_0 \cos(\omega t) + \frac{\varepsilon \tilde{\lambda}_2 a_0^2}{6\omega_0^2} (2\cos(\omega t) + \cos(2\omega t) - 3) \quad (59)$$

$$+ O(\varepsilon^2)$$

where

$$\omega = \omega_0 + \varepsilon^2 a_0^2 \left(\frac{3}{8\omega_0} \tilde{\lambda}_3 - \frac{5}{12\omega_0^3} \tilde{\lambda}_2^2 \right) \quad (60)$$

As done previously, for the above solution in Eq. (56) to be valid,

$$\frac{\varepsilon \tilde{\lambda}_2 a_0^2}{6\omega_0^2} \ll 1 \quad (61)$$

However, the analysis shows below proved otherwise

$$\lim_{\varepsilon \rightarrow \infty} \frac{\varepsilon \tilde{\lambda}_2 a_0^2}{6\omega_0^2} = \infty \gg 1 \quad (62)$$

It is shown that the above criteria in Eq. (61) for the solution provided by the classical multiple scales method cannot be achieved because of the presence of ω_0^2 being a constant in the denominator. Such constant (ω_0^2) will make the correction term to grow much larger than the leading term for

large value of (ε or $\varepsilon \rightarrow \infty$). Therefore, the solution provided by the classical multiple scales method will diverge or fail for large value of the perturbation parameter, (ε or $\varepsilon \rightarrow \infty$). This is also demonstrated in Tables 2 and 3 as well as the figures in the results and discussion sections.

3.3 Development of exact analytical solution for the nonlinear frequency

For the purpose of comparisons of results, following the procedures in ref. [80], the exact analytical solution of the nonlinear frequency is developed and given as

$$\omega = \frac{2\pi}{B} \quad (63)$$

where

$$B = \int_0^{a_0} \frac{2dq}{\sqrt{\omega_0^2 (a_0^2 - q^2) + \frac{2}{3}\varepsilon \tilde{\lambda}_2 (a_0^3 - q^3) + \frac{1}{2}\varepsilon^2 \tilde{\lambda}_3 (a_0^4 - q^4)}}$$

$$+ \int_0^{b_0} \frac{2dq}{\sqrt{\omega_0^2 (b_0^2 - q^2) - \frac{2}{3}\varepsilon \tilde{\lambda}_2 (b_0^3 - q^3) + \frac{1}{2}\varepsilon^2 \tilde{\lambda}_3 (b_0^4 - q^4)}}$$

where

$$b_0 = \frac{1}{9\varepsilon^2 \tilde{\lambda}_3} \left\{ \begin{array}{l} 4\varepsilon \tilde{\lambda}_2 + 3\varepsilon^2 a_0 \tilde{\lambda}_3 \\ + C \\ - \frac{D}{\sqrt[3]{2}} \end{array} \right\}$$

Table 2: Parameters used for simulations

S/N	Parameter	Symbol	Value
1.	Diameter of armchair single-walled nanotube	d	0.678 nm
2.	Length of the nanotube	L	6.78 nm
3.	Aspect ratio	L/h	10, 20, 50
4.	Height of the nanotube	h	0, 0.1, 0.3 nm
5.	Thickness of the nanotube	t	0.066 nm
6.	Density of the nanotube	ρ	2300 kg/m ³
7.	Young Modulus	E	5.5 TPa
8.	Poisson's ratio	ν	0.19
9.	Cross-sectional area	A	0.1406 m ²
10.	Thermal expansion coefficient for room and low Temperatures	α_x	$-1.6 \times 10^{-6} \text{ K}^{-1}$
11.	Thermal expansion coefficient for high Temperatures	α_x	$1.1 \times 10^{-6} \text{ K}^{-1}$
12.	Second moment of inertia	I	$8.155 \times 10^{-3} \text{ m}^4$
13.	Nonlocal parameter	$(e_0 a)^2$	0, 1, 2, 3, 4 nm ²
14.	Dimensionless Winkler elastic medium stiffness	K_w	0 – 50
15.	Dimensionless Pasternak elastic medium stiffness	K_p	0 – 100
16.	Dimensionless quadratic nonlinear elastic medium stiffness	K_1	0 – 100
17.	Dimensionless cubic nonlinear elastic medium stiffness	K_2	0 – 100
18.	Magnetic field permeability	η	10^3 - 10^8 N/A^2
19.	Longitudinal magnetic field	H_x	10^4 - 10^9 A/m
20.	Change in temperature	ΔT	0 – 300 K

where

$$C = \frac{\sqrt[3]{2} \left(-16\varepsilon^2 \tilde{\lambda}_2 + 12\varepsilon^2 a_0 \tilde{\lambda}_2 \tilde{\lambda}_3 + 18\varepsilon^4 a_0^2 \tilde{\lambda}_3^2 + 54\varepsilon^2 \tilde{\lambda}_3 \omega_0^2 \right)}{\sqrt{\left[\begin{array}{c} -128\varepsilon^3 \tilde{\lambda}_2^2 + 144\varepsilon^4 a_0 \tilde{\lambda}_2^2 \tilde{\lambda}_3 \\ -540\varepsilon^5 a_0^2 \tilde{\lambda}_3^2 \tilde{\lambda}_2 - 540\varepsilon^6 a_0^3 \tilde{\lambda}_3^3 \\ + 648\varepsilon^2 a \tilde{\lambda}_2 \tilde{\lambda}_3 \omega_0^2 - 972\varepsilon^4 a_0 \tilde{\lambda}_3^2 \omega_0^2 \end{array} \right] + \sqrt{\left[\begin{array}{c} 4 \left(-16\varepsilon^2 \tilde{\lambda}_2 + 12\varepsilon^2 a_0 \tilde{\lambda}_2 \tilde{\lambda}_3 \right. \\ \left. + 18\varepsilon^4 a_0^2 \tilde{\lambda}_3^2 + 54\varepsilon^2 \tilde{\lambda}_3 \omega_0^2 \right)^3 \\ + \left(-128\varepsilon^3 \tilde{\lambda}_2^2 + 144\varepsilon^4 a_0 \tilde{\lambda}_2^2 \tilde{\lambda}_3 \right. \\ \left. - 540\varepsilon^5 a_0^2 \tilde{\lambda}_3^2 \tilde{\lambda}_2 - 540\varepsilon^6 a_0^3 \tilde{\lambda}_3^3 \right. \\ \left. + 648\varepsilon^2 a \tilde{\lambda}_2 \tilde{\lambda}_3 \omega_0^2 - 972\varepsilon^4 a_0 \tilde{\lambda}_3^2 \omega_0^2 \right)^2 \end{array} \right]}}$$

$$D = \sqrt[3]{\left[\begin{array}{c} -128\varepsilon^3 \tilde{\lambda}_2^2 + 144\varepsilon^4 a_0 \tilde{\lambda}_2^2 \tilde{\lambda}_3 \\ -540\varepsilon^5 a_0^2 \tilde{\lambda}_3^2 \tilde{\lambda}_2 - 540\varepsilon^6 a_0^3 \tilde{\lambda}_3^3 \\ + 648\varepsilon^2 a \tilde{\lambda}_2 \tilde{\lambda}_3 \omega_0^2 - 972\varepsilon^4 a_0 \tilde{\lambda}_3^2 \omega_0^2 \end{array} \right] + \sqrt{\left[\begin{array}{c} 4 \left(-16\varepsilon^2 \tilde{\lambda}_2 + 12\varepsilon^2 a_0 \tilde{\lambda}_2 \tilde{\lambda}_3 \right. \\ \left. + 18\varepsilon^4 a_0^2 \tilde{\lambda}_3^2 + 54\varepsilon^2 \tilde{\lambda}_3 \omega_0^2 \right)^3 \\ + \left(-128\varepsilon^3 \tilde{\lambda}_2^2 + 144\varepsilon^4 a_0 \tilde{\lambda}_2^2 \tilde{\lambda}_3 \right. \\ \left. - 540\varepsilon^5 a_0^2 \tilde{\lambda}_3^2 \tilde{\lambda}_2 - 540\varepsilon^6 a_0^3 \tilde{\lambda}_3^3 \right. \\ \left. + 648\varepsilon^2 a \tilde{\lambda}_2 \tilde{\lambda}_3 \omega_0^2 - 972\varepsilon^4 a_0 \tilde{\lambda}_3^2 \omega_0^2 \right)^2 \end{array} \right]}}$$

3.4 Development of numerical solution

Also, the second-order ordinary differential equation in Eq. (25) was solved numerically using fifth-order Runge-Kutta-Fehlberg method (Cash-Karp Runge-Kutta). Since Runge-Kutta method is used for solving first-order ordinary differential equation, the second-order ordinary differential equation is decomposed into two first-order differential equations as follows:

$$q' = p, \quad (64a)$$

$$p' = -\frac{(\omega_0 q + \varepsilon \tilde{\lambda}_2 q^2 + \varepsilon^2 \tilde{\lambda}_3 q^3)}{\omega^2} \quad (64b)$$

Eqs. (64a) and (64b) can be written as

$$f(\tau, q, p) = p, \quad (65a)$$

$$g(\tau, q, p) = -\frac{(\omega_0 q + \varepsilon \tilde{\lambda}_2 q^2 + \varepsilon^2 \tilde{\lambda}_3 q^3)}{\omega^2}, \quad (65b)$$

The iterative scheme of the fifth-order Runge-Kutta-Fehlberg method for the system of first-order equations is given as follows:

$$q_{i+1} = q_i$$

$$+ h \left(\frac{2835}{27648} k_1 + \frac{18575}{48384} k_3 + \frac{13525}{55296} k_4 \right. \\ \left. + \frac{277}{14336} k_5 + \frac{1}{4} k_6 \right)$$

$$p_{i+1} = p_i$$

$$+ h \left(\frac{2835}{27648} l_1 + \frac{18575}{48384} l_3 + \frac{13525}{55296} l_4 \right. \\ \left. + \frac{277}{14336} l_5 + \frac{1}{4} l_6 \right)$$

where

$$k_1 = f(\tau_i, q_i, p_i)$$

$$l_1 = g(\tau_i, q_i, p_i)$$

$$k_2 = f\left(\tau_i + \frac{1}{5}h, q_i + \frac{1}{5}k_1h, p_i + \frac{1}{5}l_1h\right)$$

$$l_2 = g\left(\tau_i + \frac{1}{5}h, q_i + \frac{1}{5}k_1h, p_i + \frac{1}{5}l_1h\right)$$

$$k_3 = f\left(\tau_i + \frac{3}{10}h, q_i + \frac{3}{40}k_1h + \frac{9}{40}k_2h, p_i + \frac{3}{40}l_1h \right. \\ \left. + \frac{9}{40}l_2h\right)$$

$$l_3 = g\left(\tau_i + \frac{3}{10}h, q_i + \frac{3}{40}k_1h + \frac{9}{40}k_2h, p_i + \frac{3}{40}l_1h \right. \\ \left. + \frac{9}{40}l_2h\right)$$

$$k_4 = f\left(\tau_i + \frac{3}{5}h, q_i + \frac{3}{10}k_1h - \frac{9}{10}k_2h + \frac{6}{5}k_3h, p_i \right. \\ \left. + \frac{3}{10}l_1h - \frac{9}{10}l_2h + \frac{6}{5}l_3h\right)$$

$$l_4 = g\left(\tau_i + \frac{3}{5}h, q_i + \frac{3}{10}k_1h - \frac{9}{10}k_2h + \frac{6}{5}k_3h, p_i \right. \\ \left. + \frac{3}{10}l_1h - \frac{9}{10}l_2h + \frac{6}{5}l_3h\right)$$

$$k_5 = f\left(\tau_i + h, q_i - \frac{11}{54}k_1h + \frac{5}{2}k_2h - \frac{70}{27}k_3h \right. \\ \left. + \frac{35}{27}k_4h, p_i - \frac{11}{54}l_1h + \frac{5}{2}l_2h - \frac{70}{27}l_3h + \frac{35}{27}l_4h\right)$$

$$l_5 = g\left(\tau_i + h, q_i - \frac{11}{54}k_1h + \frac{5}{2}k_2h - \frac{70}{27}k_3h \right. \\ \left. + \frac{35}{27}k_4h, p_i - \frac{11}{54}l_1h + \frac{5}{2}l_2h - \frac{70}{27}l_3h + \frac{35}{27}l_4h\right)$$

$$k_6 = f\left(\tau_i + \frac{7}{8}h, q_i + \frac{1631}{55296}k_1h + \frac{175}{512}k_2h \right. \\ \left. + \frac{575}{13824}k_3h + \frac{44275}{110592}k_4h + \frac{253}{4096}k_5h, \right. \\ \left. p_i + \frac{1631}{55296}l_1h + \frac{175}{512}l_2h + \frac{575}{13824}l_3h \right. \\ \left. + \frac{44275}{110592}l_4h + \frac{253}{4096}l_5h, \right)$$

$$l_6 = g\left(\tau_i + \frac{7}{8}h, q_i + \frac{1631}{55296}k_1h + \frac{175}{512}k_2h \right. \\ \left. + \frac{575}{13824}k_3h + \frac{44275}{110592}k_4h + \frac{253}{4096}k_5h, \right. \\ \left. p_i + \frac{1631}{55296}l_1h + \frac{175}{512}l_2h + \frac{575}{13824}l_3h \right. \\ \left. + \frac{44275}{110592}l_4h + \frac{253}{4096}l_5h, \right)$$

Table 2 presented the parameters used for the simulations.

4 Results and discussion

The results of the analyses and parametric studies are presented in this section. The verifications of the analytical solutions are shown in Tables 3 and 4.

It could be observed from the Tables that at small values of the perturbation parameter, ε , the results of multiple scales Lindstedt-Poincare method and classical multiple scales method are almost the same and highly accurate when compared with the results of exact analytical and numerical methods. However, as the values of the perturbation parameter, ε continue to grow and become large, there are notable increasing discrepancies between the results of multiple scales Lindstedt-Poincare method and the classical multiple scales method. Moreover, for the large values of ε , $\tilde{\lambda}_2$ and $\tilde{\lambda}_3$, the analytical solutions of the multiple scales method fail, diverge much from the exact analytical and numerical solutions and provides erroneous results with large percentage errors. However, it is shown in the Tables 2 and 3 as well as in the Figures 2a-2d that for the both small and large values of ε , $\tilde{\lambda}_2$ and $\tilde{\lambda}_3$, the results of the solutions of multiple scales Lindstedt-Poincare method are in excellent agreement with the results of both exact analytical and numerical methods. It is also shown that large values of ε and $\tilde{\lambda}_3$ lead to amplitude deviation in the classical multiple scales method. However, it is observed that multiple scales Lindstedt-Poincare method produces

very good results for the large amplitudes and frequencies as well as strong nonlinearities. This shows the superiority of the Multiple scales Lindstedt-Poincare method over the classical multiple scales method which produces results of large discrepancies for strongly nonlinear systems. Therefore, the multiple scales Lindstedt-Poincare method is highly accurate and provides convergent solutions for both small and large perturbation parameters as well as for both weak and strong nonlinearities.

It should also be noted in Figures 3a and 3b that variations of $\tilde{\lambda}_2$ and $\tilde{\lambda}_3$ also depict the direct effects of the quadratic and cubic nonlinearity terms on the dynamic behaviour of the nanobeam. However, Figure 3c presents the comparison of results of linear and nonlinear dynamic responses of the nanostructure. The results show variations in the linear and nonlinear behaviour even at small values of perturbation parameter and weak nonlinearities. Moreover, as the values of the perturbation parameter and nonlinearities are increased, the variation and the discrepancies in the dynamic behaviours of the structure increase.

The Figures 4 and 5 show the deflections of the structure along its span at five different buckled and normalized mode shapes for the simple-simple and clamped-clamped supports of the nanostructure.

Figures 5–12 present the impacts of nonlocal parameter, temperature, elastic medium stiffness on the nonlinear frequency to the linear frequency ratio for both simply and clamped-clamped supported nanobeams. In all the results, it is demonstrated that as the dimensionless amplitude increases the frequency ratio increases due to the “hardening spring” behaviour of the nanobeam.

Table 3: Comparison of results of nonlinear frequency ratio when $\alpha_0 = \tilde{\lambda}_2 = \tilde{\lambda}_3 = 1$

ε ω/ω_0				
	Exact	MSM	MSLPM	% Error in MSM	% Error in MSLPM
0.1	1.000340	1.000335	1.000335	0.00049983	0.00049983
1.0	1.035926	1.033720	1.033432	0.21294957	0.24075071
10	2.954520	4.371795	2.915205	47.9697210	0.11220097
100	27.07609	338.1794	27.58255	1148.99644	1.87050641

Table 4: Comparison of results of nonlinear frequency ratio when $\alpha_0 = 1$

ε	$\tilde{\lambda}_2$	$\tilde{\lambda}_3$ ω/ω_0				% Error in MSLPM
			Exact	MSM	MSLPM	% Error in MSM	
1	1	1	1.035926	1.033720	1.033432	0.21294957	0.24075071
1	1	10	1.329955	1.375676	1.324775	3.43778549	0.51800000
1	1	100	2.890746	4.795266	2.932250	65.8833395	1.43575395
1	10	100	2.954520	4.795266	2.915205	62.3025060	1.33067300

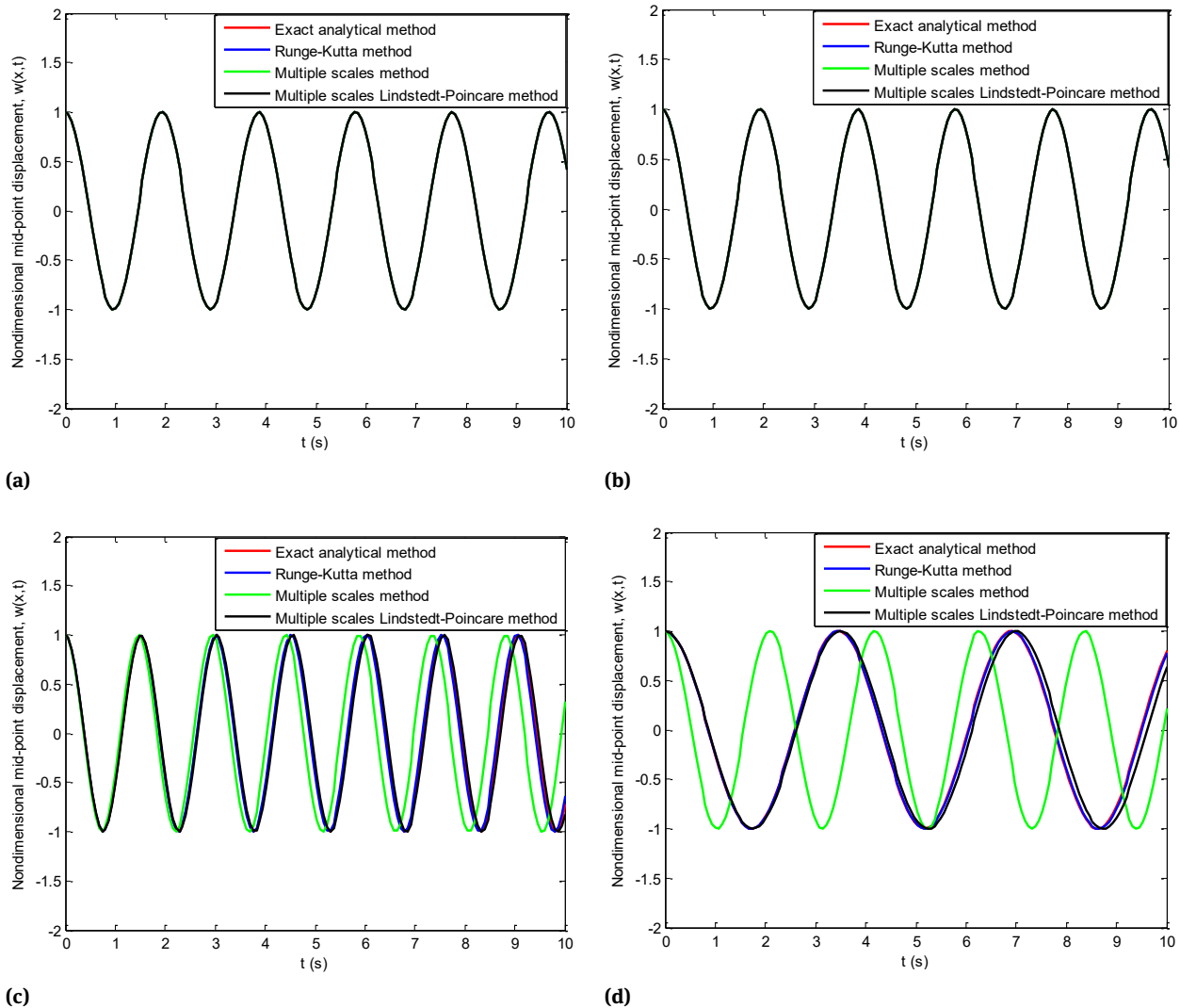


Figure 2: (a) Comparison of results when $\varepsilon = 0.1$, $a_0 = \tilde{\lambda}_2 = \tilde{\lambda}_3 = 1$, $\omega_0 = \pi$ (b) Comparison of results when $\varepsilon = a_0 = \tilde{\lambda}_2 = \tilde{\lambda}_3 = 1$, $\omega_0 = \pi$ (c) Comparison of results when $\varepsilon = a_0 = \tilde{\lambda}_2 = 1$, $\tilde{\lambda}_3 = 10$, $\omega_0 = \pi$ (d) Comparison of results when $\varepsilon = a_0 = \tilde{\lambda}_2 = 1$, $\tilde{\lambda}_3 = 100$, $\omega_0 = \pi$

Such behaviour in response to the increase in the dimensionless amplitude is caused by the increase in the axial stretching due to the large deflection which leads to a stiffer structure and a larger nonlinear frequency. The results show that at any given dimensionless amplitude, frequency ratio increases as the values of the dimensionless nonlocal, quadratic and cubic elastic medium stiffness parameters increase as shown in Figures 6–8. However, at any given dimensionless amplitude, the frequency ratio decreases as the values of the temperature change, magnetic force, Winkler and Pasternak layer stiffness parameters increase as shown in Figures 9–12. It is shown in all the figures that the impact of the dimensionless nonlocal, quadratic, cubic elastic medium stiffness, temperature change, magnetic force, Winkler and Pasternak layer stiffness parameters

on the nonlinear frequency ratio becomes significant as the dimensionless amplitude increases.

It is clearly seen that increase in temperature change at high temperature reduces the frequency ratio as shown in Figures 11. Such response is due to the fact that the Young modulus and the flexural rigidity of the nanobeam are functions of temperature. These parameters (Young modulus and the flexural rigidity) increase at high temperature and such causes the nanobeam to become increasingly rigid as the temperature change increases, which consequently decreases the frequency ratio of the vibration of the structure. However, at low or room temperature, increase in temperature change, increases the frequency ratio of the structure nanotube.

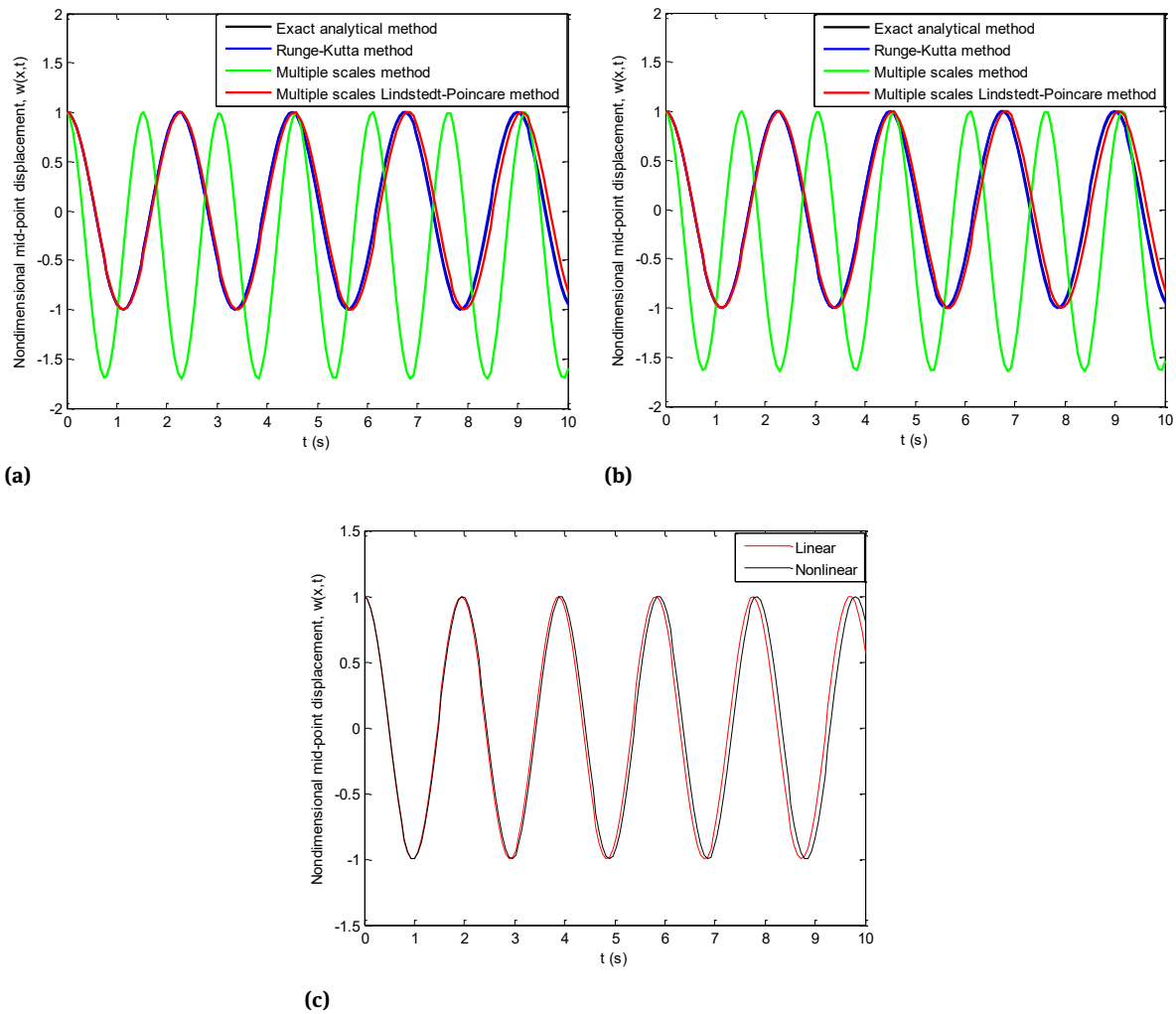


Figure 3: (a) Comparison of results when $\varepsilon = 10$, $a_0 = \tilde{\lambda}_2 = \tilde{\lambda}_3 = 1$, $\omega_0 = \pi$ (b) Comparison of results when $\varepsilon = a_0 = 1$, $\tilde{\lambda}_2 = 10$, $\tilde{\lambda}_3 = 100$, $\omega_0 = \pi$ (c) Comparison of results and effect of nonlinearity on the dynamic behaviour

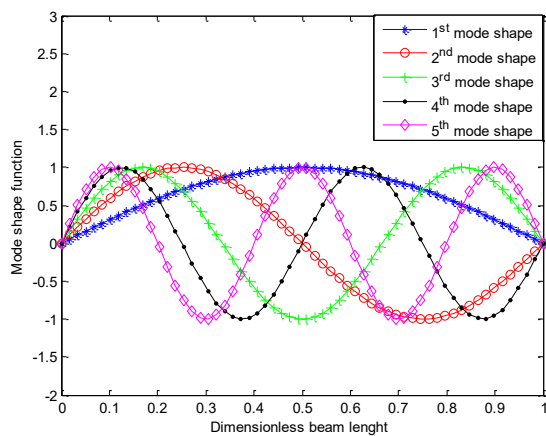


Figure 4: The first five normalized mode shaped of the beam under simple-simple supports

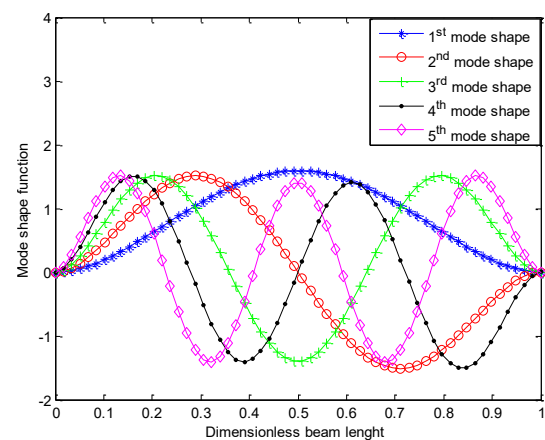


Figure 5: The first five normalized mode shaped of the beam under clamped-clamped supports

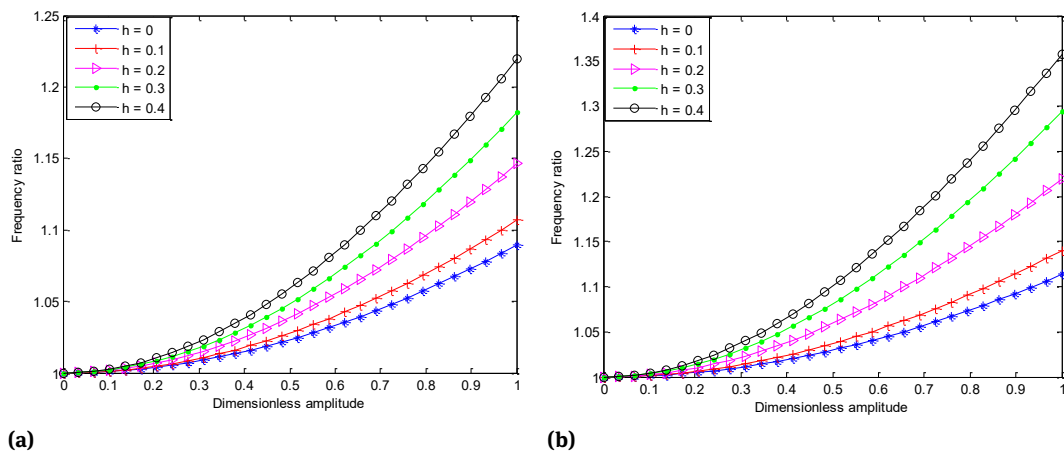


Figure 6: (a) Effects of dimensionless nonlocal parameter on the frequency ratio for simply supported nanobeam (b) Effects of dimensionless nonlocal parameter on the frequency ratio for clamped-clamped nanobeam

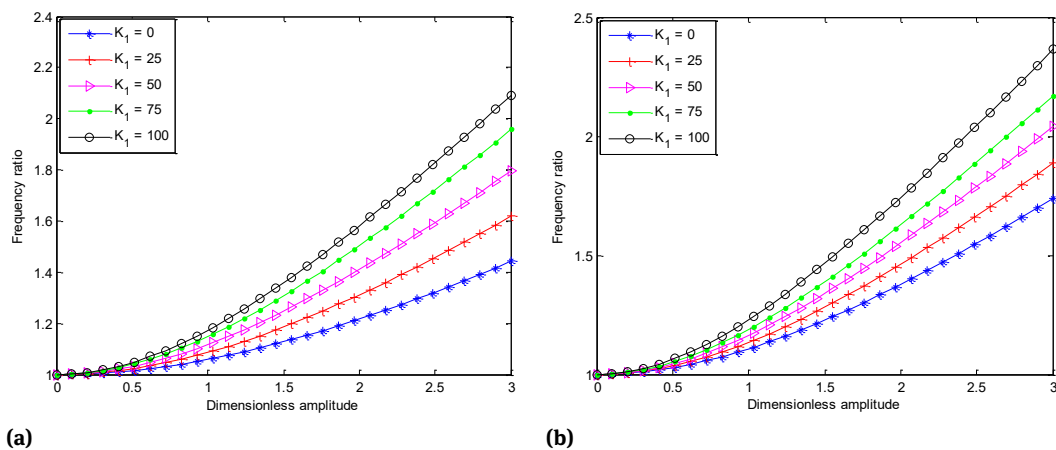


Figure 7: (a) Effects of dimensionless quadratic elastic medium stiffness on the frequency ratio for simply supported nanobeam (b) Effects of dimensionless quadratic elastic medium stiffness on the frequency ratio for clamped-clamped supported nanobeam

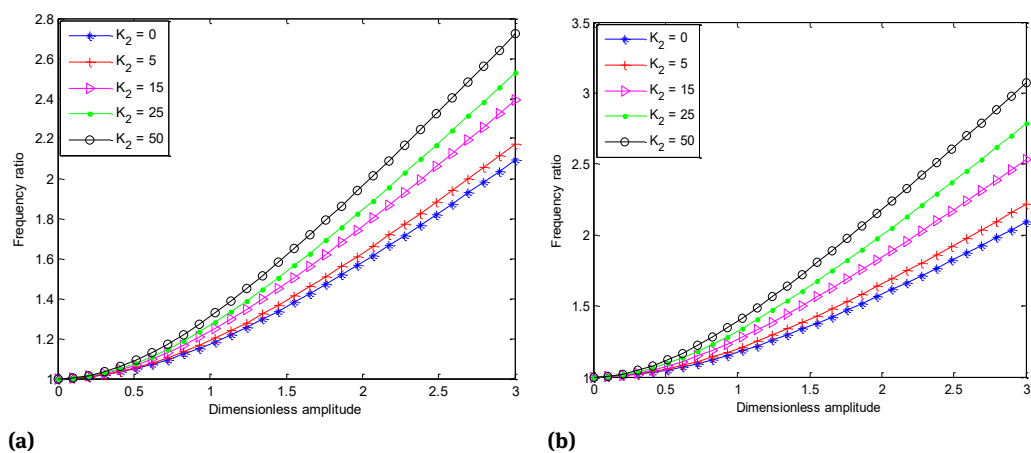


Figure 8: (a) Effects of dimensionless cubic nonlinear elastic medium stiffness on the frequency ratio for simply supported nanobeam (b) Effects of dimensionless cubic elastic medium stiffness on the frequency ratio for clamped-clamped supported nanobeam

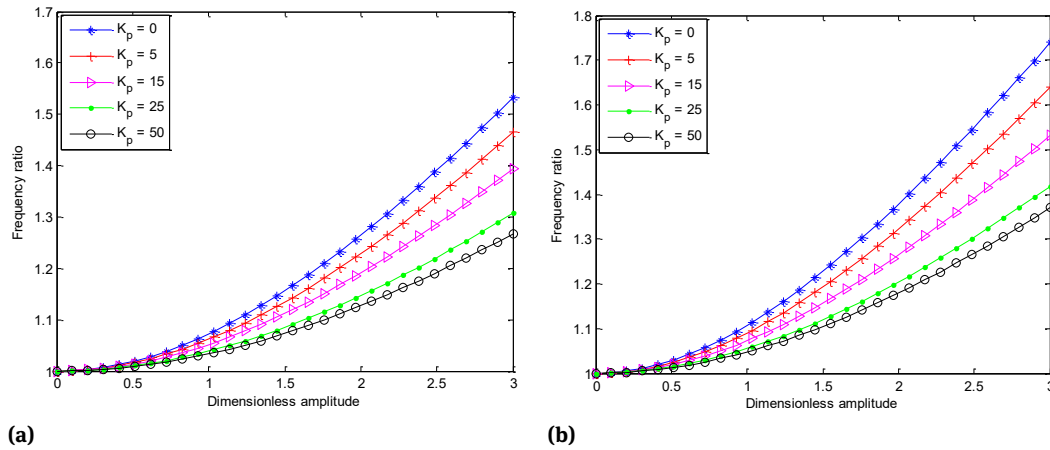


Figure 9: (a) Effects of dimensionless Pasternak elastic medium stiffness on the frequency ratio for simply supported nanobeam (b) Effects of dimensionless Pasternak elastic medium stiffness on the frequency ratio for clamped-clamped supported nanobeam

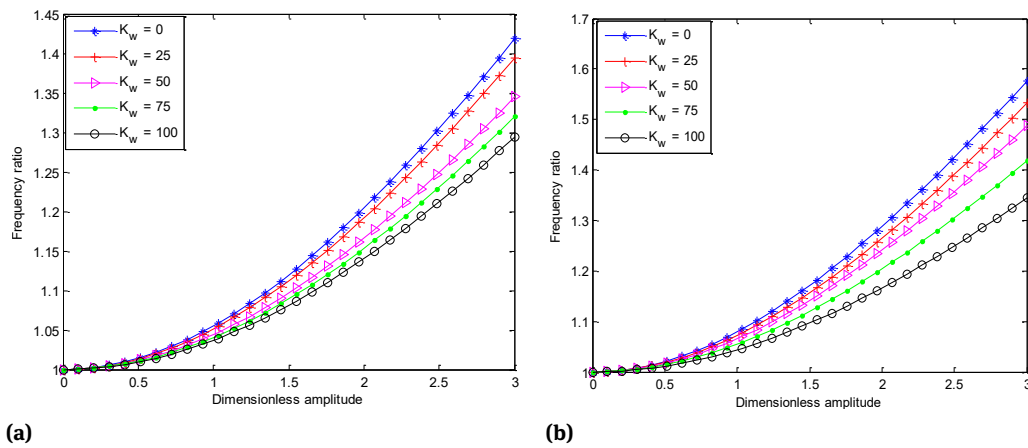


Figure 10: (a) Effects of dimensionless Winkler elastic medium stiffness on the frequency ratio for simply supported nanobeam (b) Effects of dimensionless Winkler elastic medium stiffness on the frequency ratio for clamped-clamped supported nanobeam

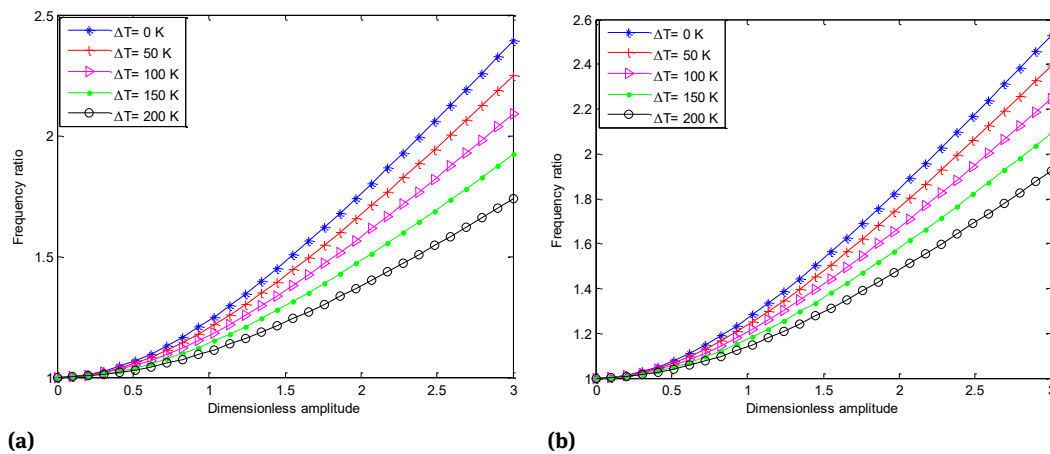


Figure 11: (a) Effects of temperature change on the frequency ratio for simply supported nanobeam (b) Effects of temperature change on the frequency ratio for clamped-clamped nanobeam

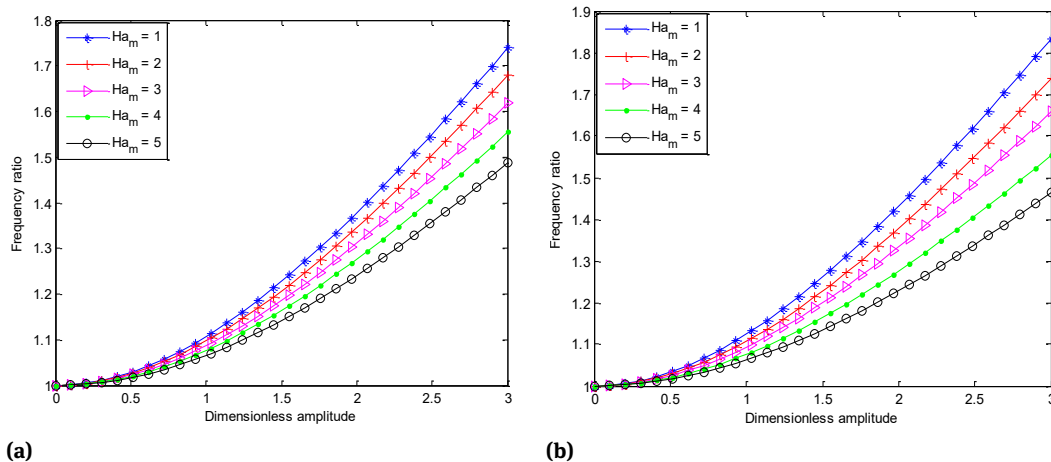


Figure 12: (a) Effects of magnetic force parameter on the frequency ratio for simply supported nanobeam (b) Effects of magnetic force parameter on the frequency ratio for clamped-clamped nanobeam

5 Conclusions

Size-dependent nonlinear vibration analysis of nanobeam embedded in multi-layer elastic media and subjected to electromechanical and thermomagnetic loadings has been presented in this work. The derivations of the nonlinear partial differential equation of motion were based on Von Karman geometric nonlinearity, nonlocal elasticity theory, Euler-Bernoulli beam theory and Hamilton's principle. From the study, the following results were established:

1. The classical multiple scales method fails and gives results with very large discrepancies from the results of the numerical and exact solutions when the perturbation parameter is large and the nonlinearity terms are strong.
2. Multiple scales Lindstedt-Poincaré method is highly efficient for strong nonlinear and large amplitude systems.
3. The frequency ratio increases as the values of the dimensionless nonlocal, quadratic and cubic elastic medium stiffness parameters increase. The dimensionless amplitude increases the frequency ratio increases.
4. The frequency ratio decreases as the values of the temperature change, magnetic force, Winkler and Pasternak layer stiffness parameters increase.
5. An increase in the temperature change at high temperature reduces the frequency ratio but at low or room temperature, increase in temperature change, increases the frequency ratio of the structure nanotube.

6. The impact of the dimensionless nonlocal, quadratic, cubic elastic medium stiffness, temperature change, magnetic force, Winkler and Pasternak layer stiffness parameters on the nonlinear frequency ratio becomes significant as the dimensionless amplitude increase.

It has also been demonstrated that the alternative computational procedures can circumvent the use and operations of other approximate analytical methods which require high skill and cost and still produce approximate analytic results of good caliber. This work will greatly benefit in the design and applications of nanobeams under electromechanical and thermomagnetic loadings.

Funding information: The author states no funding involved.

Conflict of interest: The author states no conflict of interest.

References

- [1] Iijima S. Helical micro tubes of graphitic carbon. *Nature*. 1991; 354(6348):56–8.
- [2] Terrones M, Banhart F, Grobert N, Charlier JC, Terrones H, Ajayan PM. Molecular junctions by joining single-walled carbon nanotubes. *Phys Rev Lett*. 2002 Aug; 89(7):075505.
- [3] Nagy P, Ehlich R, Biro LP, Gyjulai J. Y-branching of single walled carbon nanotubes. *Appl Phys A*. 2000; 70:481-3.
- [4] Chernozatonskii LA. Carbon nanotubes connectors and planar jungle gyms. *Appl Phys, A Mater Sci Process*. 1992; 172:173–6.

- [5] Liew KM, Wong CH, He XQ, Tan MJ, Meguid SA. Nanomechanics of single and multiwalled carbon nanotubes. *Phys Rev.* 2004; B69:115429.
- [6] Pantano A, Boyce MC, Parks DM. Mechanics of axial compression of single and multi-wall carbon nanotubes. *J Eng Mater Technol.* 2004; 126(3):279–84.
- [7] Pantano A, Parks DM, Boyce MC. Mechanics of deformation of single- and multi-wall carbon nanotubes. *J Mech Phys Solids.* 2004; 52:789–821.
- [8] Qian D, Wagner GJ, Liu WK, Yu MF, Ruoff RS. Mechanics of carbon nanotubes. *Appl Mech Rev.* 2002; 55:495–533.
- [9] Salvétat JP, Bonard JM, Thomson NH, Kulik AJ, Forro L, Benoit W, et al. Mechanical properties of carbon nanotubes. *Appl Phys, A Mater Sci Process.* 1999; A69(3):255–60.
- [10] Sears A, Batra RC. Buckling of multiwalled carbon nanotubes under axial compression. *Phys Rev.* 2006; B73:085410.
- [11] Yoon J, Ru CQ, Mioduchowski A. Noncoaxial resonance of an isolated multiwall carbon nanotube. *Phys Rev.* 2002; B66:233402.
- [12] Wang X, Cai H. Effects of initial stress on non-coaxial resonance of multi-wall carbon nanotubes. *Acta Mater.* 2006; 54(8):2067–74.
- [13] Wang CM, Tan VB, Zhang YY. Timoshenko beam model for vibration analysis of multi-walled carbon nanotubes. *J Sound Vibrat.* 2006; 294(4-5):1060–72.
- [14] Zhang Y, Liu G, Han X. Transverse vibrations of double-walled carbon nanotubes under compressive axial load. *Phys Lett A.* 2005; A340(1-4):258–66.
- [15] Elishakoff I, Pentaras D. Fundamental natural frequencies of double-walled carbon nanotubes. *J Sound Vibrat.* 2009; 322(4-5):652–64.
- [16] Buks E, Yurke B. Mass detection with a nonlinear nanomechanical resonator. *Phys Rev E Stat Nonlin Soft Matter Phys.* 2006 Oct; 74(4 Pt 2):046619.
- [17] Postma HW, Kozinsky I, Husain A, Roukes ML. Dynamic range of nanotube- and nanowire-based electromechanical systems. *Appl Phys Lett.* 2005; 86(22):86.
- [18] Fu YM, Hong JW, Wang XQ. Analysis of nonlinear vibration for embedded carbon nanotubes. *J Sound Vibrat.* 2006; 296(4-5):746–56.
- [19] Dequesnes M, Tang Z, Aluru NR. Static and dynamic analysis of carbon nanotube-based switches. *J Eng Mater Technol.* 2004; 126(3):230–237.
- [20] Ouakad HM, Younis MI. Nonlinear dynamics of electrically actuated carbon nanotube resonators. *J Comput Nonlinear Dyn.* 2010; 5(1):5.
- [21] Zamanian M, Khadem SE, Mahmoodi SN. Analysis of non-linear vibrations of a microresonator under piezoelectric and electrostatic actuations. *Proc Inst Mech Eng, C J Mech Eng Sci.* 2009; 223(2):329–44.
- [22] Belhadj A, Boukhalfa A, Belalia S. Carbon Nanotube Structure Vibration Based on Nonlocal Elasticity. *J Mod Mater.* 2016; 3(1):9–13.
- [23] Abdel-Rahman EM, Nayfeh AH. Secondary resonances of electrically actuated resonant microsensors. *J Micromech Microeng.* 2003; 13(3):491–501.
- [24] Hawwa MA, Al-Qahtani HM. Nonlinear oscillations of a double-walled carbon nanotube. *Comput Mater Sci.* 2010; 48(1):140–3.
- [25] Hajnayeb A, Khadem SE. Nonlinear vibration and stability analysis of a double-walled carbon nanotube under electrostatic actuation. *J Sound Vibrat.* 2012; 331(10):2443–56.
- [26] Xu KY, Guo XN, Ru CQ. Vibration of a double-walled carbon nanotube aroused by nonlinear intertube van der Waals forces. *J Appl Phys.* 2006; 99(6):99.
- [27] Lei XW, Natsuki T, Shi JX, Ni QQ. Surface effects on the vibrational frequency of double-walled carbon nanotubes using the nonlocal Timoshenko beam model. *Compos, Part B Eng.* 2012; 43(1):64–9.
- [28] Ghorbanpour AA, Zarei MS, Amir S, Khoddami MZ. Nonlinear nonlocal vibration of embedded DWCNT conveying fluid using shell model. *Physica B.* 2013; 410:188–96.
- [29] Ebrahimi F, Shafiei MS, Ahari MF. Vibration analysis of single and multi-walled circular graphene sheets in thermal environment using GDQM. *Waves Random Complex Media.* 2022.
- [30] Yoon J, Ru CQ, Mioduchowski A. Vibration of an embedded multiwalled carbon nanotube. *Compos Sci Technol.* 2003; 2003(63):1533–42.
- [31] Ansari R, Hemmatnezhad M. Nonlinear vibrations of embedded multi-walled carbon nanotubes using a variational approach. *Math Comput Model.* 2011; 53(5-6):927–38.
- [32] Arani AG, Rabbani H, Amir S, Maraghi ZK, Mohammadimehr M, Haghighparast E. Analysis of Nonlinear Vibrations for Multi-Walled Carbon Nanotubes Embedded in an Elastic Medium. *J Solid Mech.* 2011; 3(3):258–70.
- [33] Budarapu PR, Yb SS, Javvaji B, Mahapatra DR. Vibration analysis of multi-walled carbon nanotubes embedded in elastic medium. *Front Struct Civ Eng.* 2014; 8:151–9.
- [34] Wang CM, Tan VB, Zhang YY. Timoshenko beam model for vibration analysis of multi-walled carbon nanotubes. *J Sound Vibrat.* 2006; 294(4-5):1060–72.
- [35] Aydogdu M. Vibration of multi-walled carbon nanotubes by generalized shear deformation theory. *Int J Mech Sci.* 2008; 50(4):837–44.
- [36] Sobamowo MG. Nonlinear Vibration Analysis of Single-Walled Carbon Nanotube Conveying Fluid in Slip Boundary Conditions Using Variational Iterative Method. *J Appl Comput Mech.* 2016; 2(4):208–21.
- [37] Sobamowo MG. Nonlinear Analysis of Flow-induced Vibration in Fluid-conveying Structures using Differential Transformation Method with Cosine-Aftertreatment Technique. *Iranian Journal of Mechanical Engineering Transactions of the ISME.* 2017; 18(1):5–42.
- [38] Sobamowo MG. Nonlinear thermal and flow-induced vibration analysis of fluid-conveying carbon nanotube resting on Winkler and Pasternak foundations. *Therm Sci Eng Prog.* 2017; 4:133–49.
- [39] Sobamowo MG, Ogunmola BY, Osheku CA. Thermo-mechanical nonlinear vibration analysis of fluid-conveying structures subjected to different boundary conditions using Galerkin-Newton-Harmonic balancing method. *J Appl Comput Mech.* 2017; 3(1):60–79.
- [40] Arefi A, Nahvi H. Stability analysis of an embedded single-walled carbon nanotube with small initial curvature based on nonlocal theory. *Mech Adv Mater Struct.* 2017; 24(11):962–70.
- [41] Cigeroglu E, Samandari H. Nonlinear free vibrations of curved double walled carbon nanotubes using differential quadrature method. *Physica E.* 2014; 64:95–105.
- [42] Eringen AC. On differential equations of nonlocal elasticity and solutions of screw dislocation and surface waves. *J Appl Phys.* 1983; 54(9):4703–10.
- [43] Eringen AC. Linear theory of nonlocal elasticity and dispersion of plane waves. *Int J Eng Sci.* 1972; 10(5):425–35.

- [44] Eringen AC. Nonlocal continuum field theories. New York: Springer; 2002.
- [45] Eringen AC, Edelen DG. On nonlocal elasticity. *Int J Eng Sci.* 1972; 10(3):233–48.
- [46] Yang F, Chong A, Lam DC, Tong P. Couple stress based strain gradient theory for elasticity. *Int J Solids Struct.* 2002; 39(10):2731–43.
- [47] Park S, Gao XL. Variational formulation of a modified couple stress theory and its application to a simple shear problem. *Z Angew Math Phys.* 2008; 59(5):904–17.
- [48] Peddieson J, Buchanan GR, McNitt RP. Application of nonlocal continuum models to nanotechnology. *Int J Eng Sci.* 2003; 41(3-5):305–12.
- [49] Lu P, Lee HC, Lu C. Dynamic properties of flexural beams using a nonlocal elasticity model. *J Appl Phys.* 2006; 99(7):073510.
- [50] Reddy JN. Nonlocal theories for bending, buckling and vibration of beams. *Int J Eng Sci.* 2007; 45(2-8):288–307.
- [51] Reddy J, Pang S. Nonlocal continuum theories of beams for the analysis of carbon nanotubes. *J Appl Phys.* 2008; 103(2):023511.
- [52] Lim CW. On the truth of nanoscale for nanobeams based on nonlocal elastic stress field theory: Equilibrium, governing equation and static deflection. *Appl Math Mech – Engl Ed.* 2010; 31(1):37–54.
- [53] Lim CW. Is a nanorod (or nanotube) with a lower Young's modulus stiffer? Is not Young's modulus a stiffness indicator? *Sci China Phys Mech Astron.* 2010; 53(4):712–24.
- [54] Hosseini S, Rahmani O. Thermomechanical vibration of curved functionally graded nanobeam based on nonlocal elasticity. *J Therm Stresses.* 2016; 39(10):1252–67.
- [55] Tylikowski A. Instability of thermally induced vibrations of carbon nanotubes via nonlocal elasticity. *J Therm Stresses.* 2012; 35(1-3):281–9.
- [56] Ebrahimi F, Mahmoodi F. Vibration analysis of carbon nanotubes with multiple cracks in thermal environment. *Adv Nano Res.* 2018; 6(1):57–80.
- [57] Zhang Y, Liu X, Liu G. Thermal effect on transverse vibrations of double-walled carbon nanotubes. *Nanotechnology.* 2007; 18(44):445701.
- [58] Murmu T, Pradhan SC. Thermo-mechanical vibration of a single-walled carbon nanotube embedded in an elastic medium based on nonlocal elasticity theory. *Comput Mater Sci.* 2009 Oct; 46(4):854–9.
- [59] Karličić DZ, Jovanović D, Kozić P, Čajić M. Thermal and magnetic effects on the vibration of a cracked nanobeam embedded in an elastic medium. *J Mech Mater Struct.* 2015; 10(1):43–62.
- [60] Zarepour M, Hosseini SA, M. Zarepour M. Hosseini SA. A semi analytical method for electro-thermo-mechanical nonlinear vibration analysis of nanobeam resting on the Winkler–Pasternak foundations with general elastic boundary conditions. *Smart Mater Struct.* 2016; 25(8):085005.
- [61] Ke YL, Yang XJ, Kitipornchai S. Nonlinear free vibration of embedded double-walled carbon nanotubes based on nonlocal Timoshenko beam theory. *Comput Mater Sci.* 2009; 47(2):409–17.
- [62] Togun N. Nonlocal beam theory for nonlinear vibrations of a nanobeam resting on elastic foundation. *Bound Value Probl.* 2016; 2016(1):57.
- [63] Ansari R, Gholami R, Darabi M. Nonlinear free vibration of embedded double-walled carbon nanotubes with layerwise boundary conditions. *Acta Mech.* 2012; 223(12):2523–36.
- [64] Ma'en SS. Superharmonic resonance analysis of nonlocal nano beam subjected to axial thermal and magnetic forces and resting on a nonlinear elastic foundation. *Microsyst Technol.* 2017; 23(8):3319–30.
- [65] Murmu T, Pradha SC. Buckling analysis of a single-walled carbon nanotube embedded in an elastic medium based on nonlocal elasticity and Timoshenko beam theory and using DQM. *Physica E.* 2009; 41(7):1232–9.
- [66] Fallah A, Aghdam M. Nonlinear free vibration and post-buckling analysis of functionally graded beams on nonlinear elastic foundation. *Eur J Mech A Solids.* 2011; 30(4):571–83.
- [67] Fallah A, Aghdam M. Thermo-mechanical buckling and nonlinear free vibration analysis of functionally graded beams on nonlinear elastic foundation. *Compos B Eng.* 2012; 43(3):1523–30.
- [68] Murmu T, Pradha SC. Thermal effects on the stability of embedded carbon nanotubes. *Comput Mater Sci.* 2010; 47(3):721–6.
- [69] Soltani M, Atoufia F, Mohri F, Dimitri R, Tornabene F. Nonlocal elasticity theory for lateral stability analysis of tapered thin-walled nanobeams with axially varying materials. *Thin-walled Struct.* 2021; 159:107268.
- [70] Karami B, Janghorban M, Shahsavari D, Dimitri R, Tornabene F. Nonlocal Buckling Analysis of Composite Curved Beams Reinforced with Functionally Graded Carbon Nanotubes. *Molecules.* 2019 Jul; 24(15):E2750.
- [71] Arefi M, Bidgoli EM, Dimitri R, Tornabene F, Reddy JN. Size-dependent free vibrations of FG polymer composite curved nanobeams reinforced with graphene nanoplatelets resting on Pasternak foundations. *Appl Sci (Basel).* 2019; 9(8):1580.
- [72] Simsek M. Large amplitude free vibration of nanobeams with various boundary conditions based on the nonlocal elasticity theory. *Compos B Eng.* 2014; 56:621–28.
- [73] Pradhan SC, Murmu T. Small-Scale Effect on Vibration Analysis of Single-Walled Carbon Nanotubes Embedded in an Elastic Medium Using Nonlocal Elasticity Theory. *J Appl Phys.* 2009; 105(2):114309.
- [74] Abdullah SS, Hosseini-Hashemi S, Hussein NA, Nazemnezhad R. Thermal stress and magnetic effects on nonlinear vibration of nanobeams embedded in nonlinear elastic medium. *J Therm Stresses.* 2020; 43(10):1316–32.
- [75] He JH. Modified Lindstedt-Poincare methods for some strongly nonlinear oscillations. Part I: expansion of a constant. *Int J Nonlinear Mech.* 2002; 37:309–14.
- [76] He JH. Modified Lindstedt-Poincare methods for some strongly nonlinear oscillations. Part II: a new transformation. *Int J Nonlinear Mech.* 2002; 37:315–20.
- [77] Marinca V, Herisanu N. A modified iteration perturbation method for some nonlinear oscillation problems. *Acta Mech.* 2006; 184(1-4):231–42.
- [78] Pakdemirli M, Karahan MM, Boyacı H. A new perturbation algorithm with better convergence properties: Multiple Scales Lindstedt-Poincare Method. *Math Comput Appl.* 2009; 14(1):31–44.
- [79] Pakdemirli M. A comparison of two perturbation methods for vibrations of systems with quadratic and cubic nonlinearities. *Mech Res Commun.* 1994; 21(2):203–8.
- [80] Pakdemirli M, Karahan MM. A new perturbation solution for systems with strong quadratic and cubic nonlinearities. *Math Methods Appl Sci.* 2010; 33(6):704–12.

APPENDIX

Following the nonlocal theory presented by Erigen [42–44] and that of Erigen and Edelen [45], the relationship between the nonlocal stress-tensor (σ_{ij}) at point x of an isotropic and homogenous nanobeam and the local stress-tensor (t_{ij}) is

$$\left[1 - (e_0 a)^2 \nabla^2\right] \sigma_{ij} = \left[1 - (\tau l)^2 \nabla^2\right] \sigma_{ij} = E \varepsilon(x) = t_{ij} \quad (\text{A1})$$

Algebraically, Eq. (A1) can be written as

$$\sigma_{xx} - (e_0 a)^2 \frac{\partial^2 \sigma_{xx}}{\partial x^2} = E \varepsilon_{xx} = t_{xx} \quad (\text{A2})$$

Neglecting the damping of the nanobeam and the damping induced by the surrounding medium. Also, assuming that vibration is independent of time axial forces. Based on Euler-Bernoulli theory, the displacements in the nanobeam are given as

$$\bar{u}_1 = \bar{u}(\bar{x}, \bar{t}) - \bar{z} \frac{\partial \bar{w}}{\partial \bar{x}}; \quad \bar{u}_2 = \bar{w}(\bar{x}, \bar{t}); \quad \bar{u}_3 = 0. \quad (\text{A3})$$

$\bar{u}_3 = 0$, since, there is not any motion along the third direction.

Also, the strain in the longitudinal direction is given as

$$\varepsilon_{xx} = \frac{\partial \bar{u}_1}{\partial \bar{x}} \quad (\text{A4})$$

The strain in the longitudinal direction is related to the extension and bending strains as

$$\varepsilon_{xx} = \varepsilon_{xx}^0 + \bar{z} k; \quad (\text{A5})$$

where extension and bending strains are respectively given as

$$\varepsilon_{xx}^0 = \frac{\partial \bar{u}}{\partial \bar{x}}; \quad k = -\frac{\partial^2 \bar{w}}{\partial \bar{x}^2}. \quad (\text{A6})$$

On substituting Eq. (A6) into Eq. (A5), we have

$$\varepsilon_{xx} = \frac{\partial \bar{u}}{\partial \bar{x}} - \bar{z} \frac{\partial^2 \bar{w}}{\partial \bar{x}^2} \quad (\text{A7})$$

Considering the Von Karman geometric nonlinearity effect, the extension strain is given as

$$\varepsilon_{xx}^0 = \frac{\partial \bar{u}}{\partial \bar{x}} + \frac{1}{2} \left(\frac{\partial \bar{w}}{\partial \bar{x}} \right)^2 \quad (\text{A8})$$

Substitution of the nonlinear extension strain in Eq. (A8) and the bending strain in Eq. (A5), provides geometric nonlinearity in the longitudinal strain as

$$\varepsilon_{xx} = \frac{\partial \bar{u}}{\partial \bar{x}} + \frac{1}{2} \left(\frac{\partial \bar{w}}{\partial \bar{x}} \right)^2 - \bar{z} \frac{\partial^2 \bar{w}}{\partial \bar{x}^2} \quad (\text{A9})$$

Introducing the following stress resultants:

$$N = \int_{A_c} \sigma_{xx} dA_c; \quad M = \int_{A_c} \sigma_{xx} \bar{z} dA_c; \quad (\text{A10})$$

$$V = \int_{A_c} \sigma_{xz} dA_c; \quad I = \int_{A_c} \bar{z}^2 dA_c;$$

The required equation of motion for the nanobeam can be derived after taking the variation of the relation

$$\Pi = W + K - U \quad (\text{A11})$$

where

$$W = \int_0^L (f \bar{u} + p \bar{w}) dx \quad (\text{A12})$$

$$K = \int_0^L \left[\frac{m_0}{2} \left(\left(\frac{\partial \bar{u}}{\partial \bar{t}} \right)^2 + \left(\frac{\partial \bar{w}}{\partial \bar{t}} \right)^2 \right) + \frac{m_2}{2} \left(\frac{\partial^2 \bar{w}}{\partial \bar{x} \partial \bar{t}} \right)^2 \right] d\bar{x} \quad (\text{A13})$$

$$U = \int_V \frac{1}{2} (\sigma_{xx} \varepsilon_{xx}) dV \quad (\text{A14})$$

$$= \int_0^L \int_A \frac{E}{2} \left[\frac{\partial \bar{u}}{\partial \bar{x}} + \frac{1}{2} \left(\frac{\partial \bar{w}}{\partial \bar{x}} \right)^2 - \bar{z} \frac{\partial^2 \bar{w}}{\partial \bar{x}^2} \right]^2 dA d\bar{x}$$

Applying Hamilton's principle, the variation of Eq. (A11) is obtained as

$$\delta(\Pi) = \delta \int_0^T (W + K - U) d\bar{t} = 0 \quad (\text{A15})$$

Expansion of the RHS of Eq. (A15), gives

$$\delta(\Pi) = \delta \int_0^T (W) d\bar{t} + \delta \int_0^T (K) d\bar{t} - \delta \int_0^T (U) d\bar{t} = 0 \quad (\text{A16})$$

For the first term at the RHS of Eq. (A16), i.e. the variation of the work done by the external forces, substitution of Eq. (A12) into the first term at the RHS of Eq. (A16), provides

$$\delta \int_0^T (W) d\bar{t} = \int_0^T \int_0^L (f \delta \bar{u} + p \delta \bar{w}) d\bar{x} d\bar{t} \quad (\text{A17})$$

Also, for the second term at the RHS of Eq. (A16), i.e. the variation of the kinetic energy, substitution of Eq. (A13) into the second term at the RHS of Eq. (A16), gives

$$\delta \int_0^T (K) d\bar{t} = \int_0^T \int_0^L \left[m_0 \left(\frac{\partial \bar{u}}{\partial \bar{t}} \frac{\delta \bar{u}}{\delta \bar{t}} + \frac{\partial \bar{w}}{\partial \bar{t}} \frac{\delta \bar{w}}{\delta \bar{t}} \right) \right] d\bar{x} d\bar{t} \quad (\text{A18})$$

$$+m_2 \left(\frac{\partial^2 \bar{w}}{\partial \bar{x} \partial \bar{t}} \right) \left(\frac{\partial^2 \delta \bar{w}}{\partial \bar{x} \partial \bar{t}} \right) d\bar{x} d\bar{t}$$

Furthermore, for the third term at the RHS of Eq. (A16), i.e. the variation of the strain energy, substitution of Eq. (A14) into the third term at the RHS of Eq. (A16), results in

$$\begin{aligned} \delta \int_0^T (U) d\bar{t} &= \int_0^T \int_V \delta \left(\frac{1}{2} (\sigma_{\bar{x}\bar{x}} \varepsilon_{\bar{x}\bar{x}}) \right) dV d\bar{t} \\ &= \int_0^T \int_V \delta \left(\frac{1}{2} (E \varepsilon_{\bar{x}\bar{x}}^2) \right) dV d\bar{t} \\ &= \int_0^T \int_V \delta \left(\frac{1}{2} (\sigma_{\bar{x}\bar{x}} \delta \varepsilon_{\bar{x}\bar{x}}) \right) dV d\bar{t} \end{aligned} \quad (\text{A19})$$

Which gives

$$\begin{aligned} \delta \int_0^T (U) d\bar{t} &= \int_0^T \int_V \sigma_{\bar{x}\bar{x}} \left(\frac{\partial \delta \bar{u}}{\partial \bar{x}} + \frac{\partial \bar{w}}{\partial \bar{x}} \frac{\partial \delta \bar{w}}{\partial \bar{x}} \right. \\ &\quad \left. - z \frac{\partial^2 \delta \bar{w}}{\partial \bar{x}^2} \right) dV d\bar{t} \end{aligned} \quad (\text{A20})$$

On substituting Eq. (A10), one can write Eq. (A20) as

$$\begin{aligned} \delta \int_0^T (U) d\bar{t} &= \int_0^T \int_0^L \left[N \left(\frac{\partial \delta \bar{u}}{\partial \bar{x}} + \frac{\partial \bar{w}}{\partial \bar{x}} \frac{\partial \delta \bar{w}}{\partial \bar{x}} \right) \right. \\ &\quad \left. - M \frac{\partial^2 \delta \bar{w}}{\partial \bar{x}^2} \right] d\bar{x} d\bar{t} \end{aligned} \quad (\text{A21})$$

On substituting Eqs. (A17), (A18), and (A21) into Eq. (A16), we have

$$\begin{aligned} \delta (II) &= \int_0^T \int_0^L (f \delta \bar{u} + p \delta \bar{w}) d\bar{x} d\bar{t} \\ &\quad + \int_0^T \int_0^L \left[m_0 \left(\frac{\partial \bar{u}}{\partial \bar{t}} \frac{\partial \delta \bar{u}}{\partial \bar{t}} + \frac{\partial \bar{w}}{\partial \bar{t}} \frac{\partial \delta \bar{w}}{\partial \bar{t}} \right) \right. \\ &\quad \left. + m_2 \left(\frac{\partial^2 \bar{w}}{\partial \bar{x} \partial \bar{t}} \right) \left(\frac{\partial^2 \delta \bar{w}}{\partial \bar{x} \partial \bar{t}} \right) \right] d\bar{x} d\bar{t} \\ &\quad - \int_0^T \int_0^L \left[N \left(\frac{\partial \delta \bar{u}}{\partial \bar{x}} + \frac{\partial \bar{w}}{\partial \bar{x}} \frac{\partial \delta \bar{w}}{\partial \bar{x}} \right) - M \frac{\partial^2 \delta \bar{w}}{\partial \bar{x}^2} \right] d\bar{x} d\bar{t} = 0 \end{aligned} \quad (\text{A22})$$

According to Euler-Lagrange, the following equations are obtained

$$-m_0 \frac{\partial^2 \bar{u}}{\partial \bar{t}^2} + \frac{\partial N}{\partial \bar{x}} + f(\bar{x}, \bar{t}) = 0 \quad (\text{A23})$$

$$-m_0 \frac{\partial^2 \bar{w}}{\partial \bar{t}^2} + m_2 \frac{\partial^4 \bar{w}}{\partial \bar{x}^2 \partial \bar{t}^2} + \frac{\partial^2 M}{\partial \bar{x}^2} + p(\bar{x}, \bar{t}) \quad (\text{A24})$$

$$+ N \frac{\partial^2 \bar{w}}{\partial \bar{x}^2} = 0$$

The nonlocal axial force (nonlinear stretching force) and bending moment are given by

$$N - (e_0 a)^2 \frac{\partial^2 N}{\partial \bar{x}^2} = EA_c \left[\frac{\partial \bar{u}}{\partial \bar{x}} + \frac{1}{2} \left(\frac{\partial \bar{w}}{\partial \bar{x}} \right)^2 - \frac{\bar{N}}{EA_c} \right] - \zeta E_z A_c \quad (\text{A25})$$

$$M - (e_0 a)^2 \frac{\partial^2 M}{\partial \bar{x}^2} = EI \left(-\frac{\partial^2 \bar{w}}{\partial \bar{x}^2} \right) \quad (\text{A26})$$

After differentiating Eq. (A23) wrt \bar{x} , one arrives at

$$\frac{\partial^2 N}{\partial \bar{x}^2} = m_0 \frac{\partial^3 \bar{u}}{\partial \bar{t}^3} - \frac{\partial f}{\partial \bar{x}} \quad (\text{A27})$$

Also, from Eq. (A24), we have

$$\frac{\partial^2 M}{\partial \bar{x}^2} = -p(\bar{x}, \bar{t}) - N \frac{\partial^2 \bar{w}}{\partial \bar{x}^2} + m_0 \frac{\partial^2 \bar{w}}{\partial \bar{t}^2} - m_2 \frac{\partial^4 \bar{w}}{\partial \bar{x}^2 \partial \bar{t}^2} \quad (\text{A28})$$

Substitution of Eqs. (A27) and (A28) into Eqs. (A25) and (A26), gives the nonlocal axial force and bending moment as

$$\begin{aligned} N &= EA_c \left[\frac{\partial \bar{u}}{\partial \bar{x}} + \frac{1}{2} \left(\frac{\partial \bar{w}}{\partial \bar{x}} \right)^2 - \frac{\bar{N}}{EA_c} \right] - \zeta E_z A_c \\ &\quad + (e_0 a)^2 \left(m_0 \frac{\partial^3 \bar{u}}{\partial \bar{x} \partial \bar{t}^2} - \frac{\partial f}{\partial \bar{x}} \right) \end{aligned} \quad (\text{A29})$$

$$\begin{aligned} M &= -EI \left(\frac{\partial^2 \bar{w}}{\partial \bar{x}^2} \right) \\ &\quad + (e_0 a)^2 \left(-p - N \frac{\partial^2 \bar{w}}{\partial \bar{x}^2} + m_0 \frac{\partial^2 \bar{w}}{\partial \bar{t}^2} - m_2 \frac{\partial^4 \bar{w}}{\partial \bar{x}^2 \partial \bar{t}^2} \right) \end{aligned} \quad (\text{A30})$$

The first derivative of Eq. (A29) is given as

$$\begin{aligned} \frac{\partial N}{\partial \bar{x}} &= EA_c \left[\frac{\partial^2 \bar{u}}{\partial \bar{x}^2} + \frac{1}{2} \frac{\partial}{\partial \bar{x}} \left(\frac{\partial \bar{w}}{\partial \bar{x}} \right)^2 - \frac{\partial}{\partial \bar{x}} \left(\frac{\bar{N}}{EA_c} \right) \right] \\ &\quad - \frac{\partial}{\partial \bar{x}} (\zeta E_z A_c) + (e_0 a)^2 \left(m_0 \frac{\partial^4 \bar{u}}{\partial \bar{x}^2 \partial \bar{t}^2} - \frac{\partial^2 f}{\partial \bar{x}^2} \right) \end{aligned} \quad (\text{A31})$$

While the second derivative of Eq. (A30) provides

$$\begin{aligned} \frac{\partial^2 M}{\partial \bar{x}^2} &= -EI \left(\frac{\partial^4 \bar{w}}{\partial \bar{x}^4} \right) + (e_0 a)^2 \left(-\frac{\partial^2 p}{\partial \bar{x}^2} - N \frac{\partial^4 \bar{w}}{\partial \bar{x}^4} \right. \\ &\quad \left. + m_0 \frac{\partial^4 \bar{w}}{\partial \bar{x}^2 \partial \bar{t}^2} - m_2 \frac{\partial^6 \bar{w}}{\partial \bar{x}^4 \partial \bar{t}^2} \right) \end{aligned} \quad (\text{A32})$$

Substituting Eq. (A31) into Eq. (A23), one arrives at the horizontal equation of motion as

$$m_0 \frac{\partial^2 \bar{u}}{\partial \bar{t}^2} - EA_c \left[\frac{\partial^2 \bar{u}}{\partial \bar{x}^2} + \frac{1}{2} \frac{\partial}{\partial \bar{x}} \left(\frac{\partial \bar{w}}{\partial \bar{x}} \right)^2 \right] \quad (\text{A33})$$

$$-\frac{\partial}{\partial \bar{x}} \left(\frac{\bar{N}}{EA_c} \right) + \frac{\partial}{\partial \bar{x}} (\zeta E_z A_c) - (e_0 a)^2 \left(m_0 \frac{\partial^4 \bar{u}}{\partial \bar{x}^2 \partial \bar{t}^2} - \frac{\partial^2 f}{\partial \bar{x}^2} \right) = f(\bar{x}, \bar{t})$$

Which can also be written as

$$m_0 \frac{\partial^2 \bar{u}}{\partial \bar{t}^2} - EA_c \left[\frac{\partial^2 \bar{u}}{\partial \bar{x}^2} + \frac{1}{2} \frac{\partial}{\partial \bar{x}} \left(\frac{\partial \bar{w}}{\partial \bar{x}} \right)^2 - \frac{\partial}{\partial \bar{x}} \left(\frac{\bar{N}}{EA_c} \right) + \frac{\partial}{\partial \bar{x}} (\zeta E_z A_c) - (e_0 a)^2 \left(m_0 \frac{\partial^4 \bar{u}}{\partial \bar{x}^2 \partial \bar{t}^2} - \frac{\partial^2 f}{\partial \bar{x}^2} \right) \right] = f(\bar{x}, \bar{t}) \quad (A34)$$

where

$$\bar{N} = N_{thermal} - \eta A_c H_{\bar{x}}^2, \quad (A35)$$

$$N_{thermal} = EA_c \frac{\alpha_{\bar{x}} \Delta T}{1-2\nu} \Rightarrow \bar{N} = EA_c \frac{\alpha_{\bar{x}} \Delta T}{1-2\nu} - \eta A_c H_{\bar{x}}^2$$

Then Eq. (A29) becomes

$$N = EA_c \left[\frac{\partial \bar{u}}{\partial \bar{x}} + \frac{1}{2} \left(\frac{\partial \bar{w}}{\partial \bar{x}} \right)^2 - \frac{\left(EA_c \frac{\alpha_{\bar{x}} \Delta T}{1-2\nu} - \eta A_c H_{\bar{x}}^2 \right)}{EA_c} \right] - \zeta E_z A_c + (e_0 a)^2 \left(m_0 \frac{\partial^3 \bar{u}}{\partial \bar{x} \partial \bar{t}^2} - \frac{\partial f}{\partial \bar{x}} \right) \quad (A36)$$

Substitution of Eq. (A35) into Eq. (A34), gives the horizontal equation of motion of the nanobeam as

$$m_0 \frac{\partial^2 \bar{u}}{\partial \bar{t}^2} - EA_c \left[\frac{\partial^2 \bar{u}}{\partial \bar{x}^2} + \frac{1}{2} \frac{\partial}{\partial \bar{x}} \left(\frac{\partial \bar{w}}{\partial \bar{x}} \right)^2 - \frac{\partial}{\partial \bar{x}} \left(\frac{EA_c \frac{\alpha_{\bar{x}} \Delta T}{1-2\nu} - \eta A_c H_{\bar{x}}^2}{EA_c} \right) + \frac{\partial}{\partial \bar{x}} (\zeta E_z A_c) - (e_0 a)^2 \left(m_0 \frac{\partial^4 \bar{u}}{\partial \bar{x}^2 \partial \bar{t}^2} - \frac{\partial^2 f}{\partial \bar{x}^2} \right) \right] = f(\bar{x}, \bar{t}) \quad (A37)$$

Also, substitution of Eqs. (A32) and (A36) into Eq. (A24), provides the vertical equation of motion as

$$EI \left(\frac{\partial^4 \bar{w}}{\partial \bar{x}^4} \right) - (e_0 a)^2 \left(-\frac{\partial^2 p}{\partial \bar{x}^2} - E \left(A_c \left[\frac{\partial \bar{u}}{\partial \bar{x}} + \frac{1}{2} \left(\frac{\partial \bar{w}}{\partial \bar{x}} \right)^2 - \frac{\left(EA_c \frac{\alpha_{\bar{x}} \Delta T}{1-2\nu} - \eta A_c H_{\bar{x}}^2 \right)}{EA_c} \right] - \zeta E_z A_c + (e_0 a)^2 \left(m_0 \frac{\partial^3 \bar{u}}{\partial \bar{x} \partial \bar{t}^2} - \frac{\partial f}{\partial \bar{x}} \right) \right) \frac{\partial^4 \bar{w}}{\partial \bar{x}^4} + m_0 \frac{\partial^4 \bar{w}}{\partial \bar{x}^2 \partial \bar{t}^2} - m_2 \frac{\partial^6 \bar{w}}{\partial \bar{x}^4 \partial \bar{t}^2} \right) - p(\bar{x}, \bar{t}) - E \left(A_c \left[\frac{\partial \bar{u}}{\partial \bar{x}} + \frac{1}{2} \left(\frac{\partial \bar{w}}{\partial \bar{x}} \right)^2 - \frac{\left(EA_c \frac{\alpha_{\bar{x}} \Delta T}{1-2\nu} - \eta A_c H_{\bar{x}}^2 \right)}{EA_c} \right] - \zeta E_z A_c + (e_0 a)^2 \left(m_0 \frac{\partial^3 \bar{u}}{\partial \bar{x} \partial \bar{t}^2} - \frac{\partial f}{\partial \bar{x}} \right) \right) \frac{\partial^2 \bar{w}}{\partial \bar{x}^2} \quad (A38)$$

$$+ m_0 \frac{\partial^2 \bar{w}}{\partial \bar{t}^2} - m_2 \frac{\partial^4 \bar{w}}{\partial \bar{x}^2 \partial \bar{t}^2} = 0$$

Which can be written as

$$EI \left(\frac{\partial^4 \bar{w}}{\partial \bar{x}^4} \right) + (e_0 a)^2 \left(\frac{\partial^2 p}{\partial \bar{x}^2} + E \left(A_c \left[\frac{\partial \bar{u}}{\partial \bar{x}} + \frac{1}{2} \left(\frac{\partial \bar{w}}{\partial \bar{x}} \right)^2 - \frac{\left(EA_c \frac{\alpha_{\bar{x}} \Delta T}{1-2\nu} - \eta A_c H_{\bar{x}}^2 \right)}{EA_c} \right] - \zeta E_z A_c + (e_0 a)^2 \left(m_0 \frac{\partial^3 \bar{u}}{\partial \bar{x} \partial \bar{t}^2} - \frac{\partial f}{\partial \bar{x}} \right) \right) \frac{\partial^4 \bar{w}}{\partial \bar{x}^4} - m_0 \frac{\partial^4 \bar{w}}{\partial \bar{x}^2 \partial \bar{t}^2} + m_2 \frac{\partial^6 \bar{w}}{\partial \bar{x}^4 \partial \bar{t}^2} \right) - p(\bar{x}, \bar{t}) - E \left(A_c \left[\frac{\partial \bar{u}}{\partial \bar{x}} + \frac{1}{2} \left(\frac{\partial \bar{w}}{\partial \bar{x}} \right)^2 - \frac{\left(EA_c \frac{\alpha_{\bar{x}} \Delta T}{1-2\nu} - \eta A_c H_{\bar{x}}^2 \right)}{EA_c} \right] - \zeta E_z A_c + (e_0 a)^2 \left(m_0 \frac{\partial^3 \bar{u}}{\partial \bar{x} \partial \bar{t}^2} - \frac{\partial f}{\partial \bar{x}} \right) \right) \frac{\partial^2 \bar{w}}{\partial \bar{x}^2} + m_0 \frac{\partial^2 \bar{w}}{\partial \bar{t}^2} - m_2 \frac{\partial^4 \bar{w}}{\partial \bar{x}^2 \partial \bar{t}^2} = 0 \quad (A39)$$

where

$$p = \left(-k_w \bar{w} + k_p \frac{\partial^2 \bar{w}}{\partial \bar{x}^2} - k_2 \bar{w}^2 - k_3 \bar{w}^3 \right) \quad (A40)$$

Substitution of Eq. (A36) into Eq. (A35), gives

$$EI \left(\frac{\partial^4 \bar{w}}{\partial \bar{x}^4} \right) + (e_0 a)^2 \left(\frac{\partial^2 \left(-k_w \bar{w} - k_p \frac{\partial^2 \bar{w}}{\partial \bar{x}^2} - k_2 \bar{w}^2 - k_3 \bar{w}^3 \right)}{\partial \bar{x}^2} + E \left(A_c \left[\frac{\partial \bar{u}}{\partial \bar{x}} + \frac{1}{2} \left(\frac{\partial \bar{w}}{\partial \bar{x}} \right)^2 - \frac{\left(EA_c \frac{\alpha_{\bar{x}} \Delta T}{1-2\nu} - \eta A_c H_{\bar{x}}^2 \right)}{EA_c} \right] - \zeta E_z A_c + (e_0 a)^2 \left(m_0 \frac{\partial^3 \bar{u}}{\partial \bar{x} \partial \bar{t}^2} - \frac{\partial f}{\partial \bar{x}} \right) \right) \frac{\partial^4 \bar{w}}{\partial \bar{x}^4} - m_0 \frac{\partial^4 \bar{w}}{\partial \bar{x}^2 \partial \bar{t}^2} + m_2 \frac{\partial^6 \bar{w}}{\partial \bar{x}^4 \partial \bar{t}^2} \right) - \left(-k_w \bar{w} + k_p \frac{\partial^2 \bar{w}}{\partial \bar{x}^2} - k_2 \bar{w}^2 - k_3 \bar{w}^3 \right) - E \left(A_c \left[\frac{\partial \bar{u}}{\partial \bar{x}} + \frac{1}{2} \left(\frac{\partial \bar{w}}{\partial \bar{x}} \right)^2 - \frac{\left(EA_c \frac{\alpha_{\bar{x}} \Delta T}{1-2\nu} - \eta A_c H_{\bar{x}}^2 \right)}{EA_c} \right] - \zeta E_z A_c + (e_0 a)^2 \left(m_0 \frac{\partial^3 \bar{u}}{\partial \bar{x} \partial \bar{t}^2} - \frac{\partial f}{\partial \bar{x}} \right) \right) \frac{\partial^2 \bar{w}}{\partial \bar{x}^2} + m_0 \frac{\partial^2 \bar{w}}{\partial \bar{t}^2} - m_2 \frac{\partial^4 \bar{w}}{\partial \bar{x}^2 \partial \bar{t}^2} = 0 \quad (A41)$$

$$EI \left(\frac{\partial^4 \bar{w}}{\partial \bar{x}^4} \right) \quad (A42)$$

$$\begin{aligned}
& - (e_0 a)^2 \left(\frac{\partial^2 \left(k_w \bar{w} - k_p \frac{\partial^2 \bar{w}}{\partial \bar{x}^2} + k_2 \bar{w}^2 + k_3 \bar{w}^3 \right)}{\partial \bar{x}^2} \right. \\
& - E \left(A_c \left[\frac{\partial \bar{u}}{\partial \bar{x}} + \frac{1}{2} \left(\frac{\partial \bar{w}}{\partial \bar{x}} \right)^2 - \frac{\left(EA_c \frac{\alpha_x \Delta T}{1-2\nu} - \eta A_c H_x^2 \right)}{EA_c} \right] \right. \\
& - \zeta E_z A_c + (e_0 a)^2 \left(m_0 \frac{\partial^3 \bar{u}}{\partial \bar{x} \partial \bar{t}^2} - \frac{\partial f}{\partial \bar{x}} \right) \left. \right) \frac{\partial^4 \bar{w}}{\partial \bar{x}^4} \\
& + m_0 \frac{\partial^4 \bar{w}}{\partial \bar{x}^2 \partial \bar{t}^2} - m_2 \frac{\partial^6 \bar{w}}{\partial \bar{x}^4 \partial \bar{t}^2} \Bigg) \\
& + \left(k_w \bar{w} - k_p \frac{\partial^2 \bar{w}}{\partial \bar{x}^2} + k_2 \bar{w}^2 + k_3 \bar{w}^3 \right) \\
& - E \left(A_c \left[\frac{\partial \bar{u}}{\partial \bar{x}} + \frac{1}{2} \left(\frac{\partial \bar{w}}{\partial \bar{x}} \right)^2 - \frac{\left(EA_c \frac{\alpha_x \Delta T}{1-2\nu} - \eta A_c H_x^2 \right)}{EA_c} \right] \right. \\
& - \zeta E_z A_c + (e_0 a)^2 \left(m_0 \frac{\partial^3 \bar{u}}{\partial \bar{x} \partial \bar{t}^2} - \frac{\partial f}{\partial \bar{x}} \right) \left. \right) \frac{\partial^2 \bar{w}}{\partial \bar{x}^2} + m_0 \frac{\partial^2 \bar{w}}{\partial \bar{t}^2} \\
& - m_2 \frac{\partial^4 \bar{w}}{\partial \bar{x}^2 \partial \bar{t}^2} = 0
\end{aligned}$$

Therefore, the vertical equation of motion of the nanobeam is

$$\begin{aligned}
& EI \left(\frac{\partial^4 \bar{w}}{\partial \bar{x}^4} \right) \\
& - (e_0 a)^2 \left(k_w \frac{\partial^2 \bar{w}}{\partial \bar{x}^2} - k_p \frac{\partial^4 \bar{w}}{\partial \bar{x}^4} + k_2 \frac{\partial^2 (\bar{w}^2)}{\partial \bar{x}^2} + k_3 \frac{\partial^2 (\bar{w}^3)}{\partial \bar{x}^2} \right. \\
& - E \left(A_c \left[\frac{\partial \bar{u}}{\partial \bar{x}} + \frac{1}{2} \left(\frac{\partial \bar{w}}{\partial \bar{x}} \right)^2 - \frac{\left(EA_c \frac{\alpha_x \Delta T}{1-2\nu} - \eta A_c H_x^2 \right)}{EA_c} \right] \right. \\
& - \zeta E_z A_c + (e_0 a)^2 \left(m_0 \frac{\partial^3 \bar{u}}{\partial \bar{x} \partial \bar{t}^2} - \frac{\partial f}{\partial \bar{x}} \right) \left. \right) \frac{\partial^4 \bar{w}}{\partial \bar{x}^4} \\
& + m_0 \frac{\partial^4 \bar{w}}{\partial \bar{x}^2 \partial \bar{t}^2} - m_2 \frac{\partial^6 \bar{w}}{\partial \bar{x}^4 \partial \bar{t}^2} \Bigg) \\
& + \left(k_w \bar{w} - k_p \frac{\partial^2 \bar{w}}{\partial \bar{x}^2} + k_2 \bar{w}^2 + k_3 \bar{w}^3 \right) \\
& - E \left(A_c \left[\frac{\partial \bar{u}}{\partial \bar{x}} + \frac{1}{2} \left(\frac{\partial \bar{w}}{\partial \bar{x}} \right)^2 - \frac{\left(EA_c \frac{\alpha_x \Delta T}{1-2\nu} - \eta A_c H_x^2 \right)}{EA_c} \right] \right. \\
& - \zeta E_z A_c + (e_0 a)^2 \left(m_0 \frac{\partial^3 \bar{u}}{\partial \bar{x} \partial \bar{t}^2} - \frac{\partial f}{\partial \bar{x}} \right) \left. \right) \frac{\partial^2 \bar{w}}{\partial \bar{x}^2} + m_0 \frac{\partial^2 \bar{w}}{\partial \bar{t}^2} \\
& - m_2 \frac{\partial^4 \bar{w}}{\partial \bar{x}^2 \partial \bar{t}^2} = 0
\end{aligned} \tag{A43}$$

Taking $m_0 = \rho A_c$, neglecting the rotary inertial (i.e. $m_2 = 0$) with no axial distributed force (i.e. $f(\bar{x}, \bar{t}) = 0$) and zero axial displacements (i.e. $\bar{u} = 0$). After some mathematical processes of Integrating the nonlinear stretching force, N between the limits 0 and L and applying the boundary con-

ditions $\bar{u}(0, t)$ and $\bar{u}(L, t)$ makes the axial normal force in Eq. (A36) to become

$$\begin{aligned}
N = & \left(\frac{EA_c}{2L} \int_0^L \left(\frac{\partial \bar{w}}{\partial \bar{x}} \right)^2 d\bar{x} \right) \\
& - \left(EA_c \frac{\alpha_x \Delta T}{1-2\nu} - \eta A_c H_x^2 \right) - \zeta E_z A_c
\end{aligned} \tag{A44}$$

That is

$$\begin{aligned}
& EA_c \left[\frac{\partial \bar{u}}{\partial \bar{x}} + \frac{1}{2} \frac{\partial}{\partial \bar{x}} \left(\frac{\partial \bar{w}}{\partial \bar{x}} \right)^2 \right. \\
& - \left. \frac{\left(EA_c \frac{\alpha_x \Delta T}{1-2\nu} - \eta A_c H_x^2 \right)}{EA_c} \right] - \zeta E_z A_c \\
& + (e_0 a)^2 \left(m_0 \frac{\partial^3 \bar{u}}{\partial \bar{x} \partial \bar{t}^2} - \frac{\partial f}{\partial \bar{x}} \right) = \left(\frac{EA_c}{2L} \int_0^L \left(\frac{\partial \bar{w}}{\partial \bar{x}} \right)^2 d\bar{x} \right) \\
& - \left(EA_c \frac{\alpha_x \Delta T}{1-2\nu} - \eta A_c H_x^2 \right) - \zeta E_z A_c
\end{aligned} \tag{A45}$$

Therefore, Eq. (A37) and (A43) reduce to

$$\begin{aligned}
& EI \left(\frac{\partial^4 \bar{w}}{\partial \bar{x}^4} \right) + \rho A_c \frac{\partial^2}{\partial \bar{t}^2} \left[\bar{w} - (e_0 a)^2 \frac{\partial^2 \bar{w}}{\partial \bar{x}^2} \right] \\
& + k_w \left[\bar{w} - (e_0 a)^2 \frac{\partial^2 \bar{w}}{\partial \bar{x}^2} \right] - k_p \frac{\partial^2}{\partial \bar{x}^2} \left[\bar{w} - (e_0 a)^2 \frac{\partial^2 \bar{w}}{\partial \bar{x}^2} \right] \\
& + k_2 \left[\bar{w}^2 - (e_0 a)^2 \frac{\partial^2 (\bar{w}^2)}{\partial \bar{x}^2} \right] + k_3 \left[\bar{w}^3 - (e_0 a)^2 \frac{\partial^2 (\bar{w}^3)}{\partial \bar{x}^2} \right] \\
& - \eta A_c H_x^2 \frac{\partial^2}{\partial \bar{x}^2} \left[\bar{w} - (e_0 a)^2 \frac{\partial^2 \bar{w}}{\partial \bar{x}^2} \right] \\
& + \left(EA_c \frac{\alpha_x \Delta T}{1-2\nu} \right) \frac{\partial^2}{\partial \bar{x}^2} \left[\bar{w} - (e_0 a)^2 \frac{\partial^2 \bar{w}}{\partial \bar{x}^2} \right] \\
& + \zeta E_z A_c \frac{\partial^2}{\partial \bar{x}^2} \left[\bar{w} - (e_0 a)^2 \frac{\partial^2 \bar{w}}{\partial \bar{x}^2} \right] \\
& - \left[\left(\frac{EA_c}{2L} \int_0^L \left(\frac{\partial \bar{w}}{\partial \bar{x}} \right)^2 d\bar{x} \right) \left(\frac{\partial^2 \bar{w}}{\partial \bar{x}^2} - (e_0 a)^2 \frac{\partial^4 \bar{w}}{\partial \bar{x}^4} \right) \right] = 0
\end{aligned} \tag{A46}$$